

## Pion condensation and realistic interactions

W. H. Dickhoff

*Natuurkundig Laboratorium, Vrije Universiteit Amsterdam, Amsterdam, Netherlands*

Amand Faessler

*Institut für Theoretische Physik, Universität Tübingen, D-7400 Tübingen, West Germany*

J. Meyer-ter-Vehn\* and H. Mütter

*Institut für Kernphysik, Kernforschungsanlage Jülich, D-5170 Jülich, West Germany*

(Received 31 March 1980)

The static pion  $p$ -wave self-energy in symmetric nuclear matter is calculated, taking into account the effects of nucleon particle-hole (ph) and  $\Delta$ -isobar nucleon-hole ( $\Delta h$ ) states. The residual interaction between ph states is derived from a Brueckner  $G$  matrix which depends on the starting energy and three momentum variables. The coupling of ph and  $\Delta h$  states and the  $\Delta h$ - $\Delta h$  interaction is described by  $\pi$  and  $\rho$  exchange taking into account the effects of  $NV$  correlations. The resulting self-energies are analyzed in the model of constant interaction strengths which is commonly used. This analysis yields effective interaction strengths weakly depending on the momentum of the pion field as well as on the nuclear density. Only in the limit of vanishing pion momentum the strength of the ph interaction is connected with the Landau parameter  $G_0'$ . The present calculation yields pion condensation at twice the empirical nuclear matter density when isobars are included.

[NUCLEAR STRUCTURE Particle-hole interaction, nuclear matter. Brueckner  $G$  matrix, isobar configurations, pion condensation.]

### I. INTRODUCTION

The occurrence of pion condensation in a nuclear medium has important consequences for various nuclear systems. The cooling rate of neutron stars, for example, increases drastically when a pion condensate is present<sup>1</sup>; even the envelope might be blown off once the central density of a neutron star reaches the critical value for pion condensation.<sup>2</sup> In relativistic heavy ion collisions, where the nuclear system is compressed, pionic instabilities may show up although the system is highly excited.<sup>3</sup> There also exists the possibility of the formation of superdense nuclei due to pion condensates.<sup>4</sup> Although unnatural parity states of normal nuclei indicate that there are no pion condensates present in finite nuclei,<sup>5</sup> it has been pointed out that precritical phenomena may occur due to proximity to pion condensation.<sup>6,7</sup> Their occurrence critically depends on baryonic interactions in the pion channel. It is these interactions which are investigated in the present paper.

Threshold to pion condensation in isospin symmetric nuclear matter is characterized by a double pole of the pion propagator<sup>8</sup>

$$D(\vec{k}, \omega; \rho) = [\omega^2 - k^2 - m_\pi^2 - \Pi(\vec{k}, \omega; \rho)]^{-1} \quad (1.1)$$

at  $\omega = 0$ , where  $\vec{k}, \omega$  is the four-momentum of the pion,  $\rho$  the density of nuclear matter, and  $\Pi$  the proper self-energy of the pion. Units are such that  $\hbar = c = 1$ . The density at which the double pole

occurs is called the critical density  $\rho_{crit}$ . The pion propagator obeys the relation

$$D(\vec{k}, \omega; \rho) = D_0(\vec{k}, \omega) + D_0(\vec{k}, \omega)\Pi(\vec{k}, \omega; \rho)D(\vec{k}, \omega; \rho), \quad (1.2)$$

where  $D_0$  is the free pion Green's function. It is the pion self-energy  $\Pi$  which will be calculated in the following. Since we restrict ourselves to symmetric nuclear matter in this paper, only the  $p$ -wave self-energy is considered; the contribution from  $s$ -wave interaction is assumed to be negligible.

Since the first papers on the possibility of pion condensation<sup>9,10</sup> have been published, much work has been devoted to the calculation of the threshold density in nuclear and neutron matter, and we refer to the review articles by Brown and Weise,<sup>11</sup> Migdal,<sup>12</sup> and Bäckman and Weise.<sup>8</sup> For finite nuclei also, this problem has been investigated.<sup>7,13-15</sup> In all calculations the results show a great sensitivity to details of the effective interactions in the pion channel including nucleon particle-hole (ph) as well as  $\Delta$ -isobar nucleon-hole ( $\Delta h$ ) interaction. In most calculations these interactions have been represented by a constant model interaction of the form  $g' \vec{\sigma}_1 \cdot \vec{\sigma}_2 \vec{\tau}_1 \cdot \vec{\tau}_2$ , familiar from the Landau-Migdal theory of Fermi liquids although in the context of pion condensation one is far from the Landau limit ( $k \rightarrow 0$ ), but needs the interactions for  $k \sim k_F$ , where  $k_F$  is the Fermi momentum. A real-

istic interaction as used in this work is far from being constant even in the Landau limit, where it still strongly depends on the angle between the relative ph momenta in the initial and final states. Thus the main point of the present paper is to determine how far the assumption of constant interactions affects the results.

The present investigation goes beyond earlier work by Bertsch and Johnson<sup>16</sup> and that of Bäckman, Brown, and Weise<sup>17,18</sup> in that it keeps the full complexity of the interactions depending on three-momenta, energy, and density when calculating the pion self-energy in nuclear matter. For the nucleon particle-hole interaction, a Brueckner  $G$  matrix derived from a realistic nucleon-nucleon ( $NN$ ) interaction<sup>19,20</sup> is transformed into the ph channel; the  $\Delta$ -isobar nucleon-hole interactions are derived from  $\pi$  and  $\rho$  meson exchange potentials taking into account  $NN$  correlations.

The formalism considering only intermediate nucleon ph states is derived in Sec. II A. Detailed formulas for the calculation of the ph residual in-

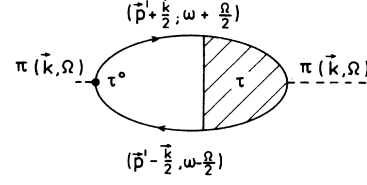


FIG. 1. Pion self-energy due to nucleon particle-hole excitations [see Eq. (2.1)].

teraction are given in Appendix A. Section II A, and with some more details Appendix B also, contain a discussion of the energy dependence of the ph interaction. To take into account effects from  $\Delta$ -isobar configurations the formalism is extended in Sec. II B. The residual interactions between ph and  $\Delta$ -isobar nucleon-hole ( $\Delta h$ ) states are discussed in Sec. III. Results for the pion self-energy are presented in Sec. IV and analyzed in the simple model of constant interaction strengths. The final section contains some conclusions of the present work.

## II. STATIC PION SELF-ENERGY IN NUCLEAR MATTER

### A. Nucleons only

In this section, we consider the pion  $p$ -wave self-energy due to the interaction with nucleons in the static limit ( $\Omega=0$ ). The corresponding Feynman diagram (see Fig. 1) is given by

$$\Pi_N(k, \Omega=0) = \sum_{TSM_S} \int \frac{d\omega}{2\pi i} \int \frac{d^3p}{(2\pi)^3} \tau^0(TSM_S k) g\left(\vec{p} + \frac{\vec{k}}{2}, \omega\right) g\left(\vec{p} - \frac{\vec{k}}{2}, \omega\right) \tau(TSM_S \vec{p}, \omega; k) \quad (2.1)$$

with the bare pion nucleon vertex

$$\begin{aligned} \tau^0(TSM_S, k) &= \sum_{t_1 t_2} \sum_{s_1 s_2} (-)^{1/2-t_2} \langle \frac{1}{2}t_1, \frac{1}{2} - t_2 | TM_T \rangle (-)^{1/2-s_2} \langle \frac{1}{2}s_1, \frac{1}{2} - s_2 | SM_S \rangle \left\langle \frac{1}{2}t_1, \frac{1}{2}s_1 \left| \frac{f_\pi \Gamma(k)}{m_\pi} \vec{\sigma} \cdot \vec{k} \tau_z \right| \frac{1}{2}t_2, \frac{1}{2}s_2 \right\rangle \\ &= \frac{f_\pi \Gamma(k)}{m_\pi} \cdot 2k \delta_{T,1} \delta_{S,1} \delta_{M_S,0}. \end{aligned} \quad (2.2)$$

Here  $f_\pi$  denotes the pion-nucleon coupling constant,  $m_\pi$  the pion mass, and  $\Gamma(k)$  a form factor. The values of all the coupling constants, masses, and cutoff masses in form factors used in the calculation are given in Appendix A. Note that without any loss of generality we restrict ourselves to the  $\pi^0$  self-energy. The ph pair carries the quantum numbers of the pion  $T=1$ ,  $S=1$ , and  $M_S=0$ , where  $M_S$  refers to the direction of the pion momentum  $k$  which serves as the polar axis in the following. The momentum  $k$  is also equal to the total ph momentum. For spin and isospin symmetric nuclear matter, the Green's function in Eq. (2.1) for nucleons near the Fermi surface may be written as

$$g(\vec{p}, \omega) = \frac{Z_p}{\omega - \epsilon_p + i\eta \operatorname{sgn}(\epsilon_p - \epsilon_F)} + g_R(\vec{p}, \omega), \quad (\eta=+0) \quad (2.3)$$

where the first term gives the pole part of the single-particle (s.p.) propagator with the s.p. energy  $\epsilon_p$ , the Fermi energy  $\epsilon_F$ , the s.p. strength  $Z_p$ , and  $g_R(\vec{p}, \omega)$  is a background term which is weakly dependent on energy. It is well known<sup>21</sup> that  $Z_p$  and  $g_R$  renormalize the ph interaction and s.p. vertices such as  $\tau^{(0)}$  (reducing its strength). For simplicity, we shall set  $Z_p=1$  and  $g_R=0$  for all momenta  $P$  throughout this work, keeping in mind that our final results for  $\Pi_N$  will be somewhat too large due to this approximation.

The vertex  $\tau(\vec{p}, \omega; k)$  in Eq. (2.1) is determined by the integral equation

$$\tau(T=1, S=1, M_S=0, \vec{p}, \omega; k) = \tau^0(110k) + \int \frac{d\omega'}{2\pi i} \int \frac{d^3p'}{(2\pi)^3} \bar{G}_{110}(\vec{p}, \vec{p}'; k, \omega + \omega') \times g\left(\vec{p}' + \frac{\vec{k}}{2}, \omega'\right) g\left(\vec{p}' - \frac{\vec{k}}{2}, \omega'\right) \tau(110\vec{p}', \omega'; k), \quad (2.4)$$

which is displayed graphically in Fig. 2.

The square interaction block  $\bar{G}$  is a central quantity of interest in this paper. It represents all interactions between the particle and hole lines irreducible with respect to vertical ph cuts and one-pion cuts. We shall approximate  $\bar{G}$  by a Brueckner  $G$  matrix obtained from the nucleon-nucleon interaction (see Sec. IIIA) and subtract direct static one-pion exchange (see also Fig. 3):

$$\bar{G}_{110}(\vec{p}, \vec{p}'; k, \omega + \omega') \cong G_{110}(\vec{p}, \vec{p}'; k, E = \omega + \omega') + \left(\frac{f_\pi \Gamma}{m_\pi}\right)^2 \frac{4k^2}{m_\pi^2 + k^2}. \quad (2.5)$$

The explicit transformation of  $G$  from the particle-particle into the particle-hole channel is derived in Appendix A. There it is shown that the interaction does not couple different  $(TSM_S)$  channels, at least not for nucleon ph channels. Therefore we suppress these spin-isospin indices in the following.

The  $G$  matrix sums all the ladder diagrams in the particle-particle direction, and its starting energy  $E = \omega + \omega'$  is clearly the sum of the energies of the incoming lines. Concerning the analytical structure of  $G(E)$ , it has poles which lie in the lower half of the energy plane ( $\text{Im}E_{\text{pole}} < 0$ ). Having this in mind, the energy integration in Eq. (2.4) is performed by closing the integration path through the upper half plane, obtaining

$$\tau(\vec{p}, \omega; k) = \tau^0(k) + P \int \frac{d^3p'}{(2\pi)^3} \left[ \frac{\bar{G}(\vec{p}, \vec{p}'; k, \omega + \epsilon_{|\vec{p}' + \vec{k}/2|}) n(|\vec{p}' + \vec{k}/2|)}{\epsilon_{|\vec{p}' + \vec{k}/2|} - \epsilon_{|\vec{p}' - \vec{k}/2|}} \tau(\vec{p}', \epsilon_{|\vec{p}' + \vec{k}/2|}; k) + \frac{\bar{G}(\vec{p}, \vec{p}'; k, \omega + \epsilon_{|\vec{p}' - \vec{k}/2|}) n(|\vec{p}' - \vec{k}/2|) \tau(\vec{p}', \epsilon_{|\vec{p}' - \vec{k}/2|}; k)}{\epsilon_{|\vec{p}' - \vec{k}/2|} - \epsilon_{|\vec{p}' + \vec{k}/2|}} \right], \quad (2.6)$$

where  $n(|\vec{q}|) = \Theta(p_F - |\vec{q}|)$  is a step function confining  $\vec{q}$  to the interior of the Fermi sphere. The two terms under the integral in Eq. (2.6) are related by the transformation  $\vec{k} \rightarrow -\vec{k}$  or, alternatively, by a reflection  $U$  of the vector  $\vec{p}'$  in the  $(x, y)$  plane keeping  $k$  fixed as the polar  $z$  axis:

$$U\vec{p}' \equiv U(p', \Theta', \phi') = (p', \pi - \Theta', \phi'). \quad (2.7)$$

One finds  $|U\vec{p}' \mp \vec{k}/2| = |\vec{p}' \pm \vec{k}/2|$ . Shifting in addition  $(\vec{p}' \pm \vec{k}/2) \rightarrow \vec{p}'$  and setting  $\omega = \epsilon_{|\vec{p}' \pm \vec{k}/2|}$ , one obtains

$$\tau(\vec{p}, \epsilon_{|\vec{p}' \pm \vec{k}/2|}; k) = \tau^0(k) + P \int \frac{d^3p'}{(2\pi)^3} \frac{1}{\epsilon_{p'} - \epsilon_{|\vec{p}' \pm \vec{k}|}} \times \left[ \bar{G}(\vec{p}, \vec{p}' - \vec{k}/2; k, \epsilon_{|\vec{p}' + \vec{k}/2|} + \epsilon_{p'}) \tau(\vec{p}' - \vec{k}/2, \epsilon_{p'}; k) + \bar{G}(\vec{p}, U(\vec{p}' - \vec{k}/2); k, \epsilon_{|\vec{p}' + \vec{k}/2|} + \epsilon_{p'}) \tau(U(\vec{p}' - \vec{k}/2), \epsilon_{p'}; k) \right], \quad (2.8)$$

where the integration now extends over the Fermi sphere  $F$  as indicated by the solid circle in Fig. 4. The total integration space splits into the  $R$  region corresponding to particle-hole states and the  $S$  region corresponding to hole-hole states.

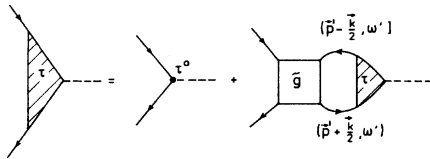


FIG. 2. Graphical representation of the integral equation (2.4) to calculate the dressed pion vertex  $\tau$  [see Eq. (2.4)].

The latter contribute due to the energy dependence of the interaction. In terms of time-ordered diagrams, hole-hole intermediate states occur between time-overlapping  $G$ -matrix blocks as shown in Fig. 5. In our representation of the interaction

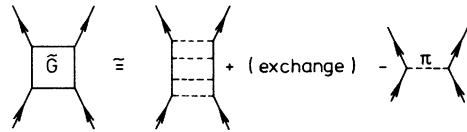


FIG. 3. Graphical representation of the interaction block  $\bar{G}$  as it is approximated in the present calculations [see Eq. (2.5)].

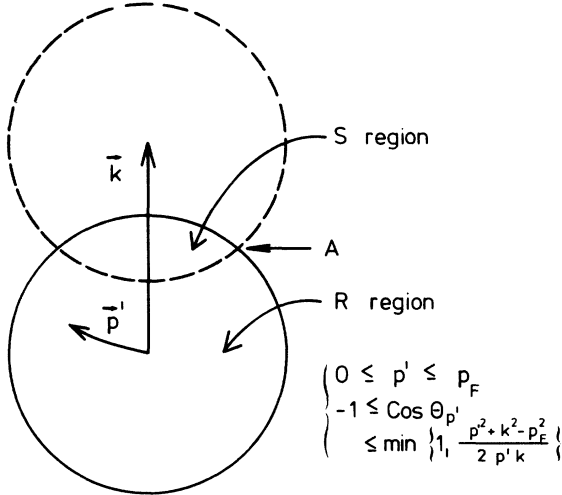


FIG. 4. The space for momentum integration in the integral equation (2.8).

the time structure is represented by an energy dependence of the  $G$  matrix. If this energy dependence is neglected in Eq. (2.6) the contribution from the intermediate hole-hole states which corresponds to the  $S$  region of Fig. 4, vanishes, since then there are no poles in the  $\text{Im}\omega < 0$  plane. Since the actual energy dependence of  $G(E)$  is weak and smooth, one can expand around an average energy  $E_0$

$$G(E) = G(E_0) \cdot [1 + \alpha(E - E_0) + \dots]. \quad (2.9)$$

It is now convenient to determine  $E_0$  such that the term  $\alpha \cdot (E - E_0)$  gives no contribution to the final results  $\Pi_N(k)$ , at least approximately. It is shown in Appendix B that this condition leads to

$$E_0 = 2 \int_{\mathcal{R}} \frac{d^3 p}{(2\pi)^3} \frac{\epsilon_p}{\epsilon_p - \epsilon_{|\vec{p}-\vec{k}|}} \bigg/ \int_{\mathcal{R}} \frac{d^3 p}{(2\pi)^3} \frac{1}{\epsilon_p - \epsilon_{|\vec{p}-\vec{k}|}}. \quad (2.10)$$

In the following, we replace the energy dependence in Eq. (2.8) by the average starting energy  $E_0$ . Thereby we account for the energy dependence in a good approximation, but avoid dealing with it explicitly

Introducing the quantity

$$\sigma(\vec{p}, k) = \frac{1}{2\tau^0(k)} (\tau(\vec{p} - \vec{k}/2, \epsilon_p; k) + \tau(U(\vec{p} - \vec{k}/2), \epsilon_p; k)), \quad (2.11)$$

the integral equation (2.8) is now obtained in the form

$$\sigma(\vec{p}, k) = 1 + \int_{\mathcal{R}} \frac{d^3 p'}{(2\pi)^3} K(\vec{p}, \vec{p}'; k) \frac{1}{\epsilon_{p'} - \epsilon_{|\vec{p}'-\vec{k}|}} \sigma(\vec{p}', k), \quad (2.12)$$

where

$$K(\vec{p}, \vec{p}'; k) = \tilde{G}(\vec{p} - \vec{k}/2, \vec{p}' - \vec{k}/2; k, E_0) + \tilde{G}(\vec{p} - \vec{k}/2, U(\vec{p}' - \vec{k}/2); k, E_0) \quad (2.13)$$

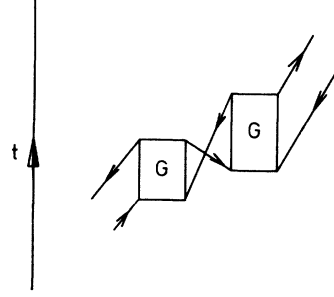


FIG. 5. Contribution to the integral equation (2.8) from the region  $S$  due to the energy dependence or the time structure of the  $G$  matrix.

and the symmetry (derived in Appendix A)

$$G(\vec{p}, \vec{p}'; k, E_0) = G(U\vec{p}, U\vec{p}'; k, E_0) \quad (2.14)$$

has been used. The integration in Eq. (2.12) is restricted to the  $R$  region; contributions from the  $S$  region cancel. This is important since the singularity at  $\epsilon_{|\vec{p}'|=1} = \epsilon_{|\vec{p}'-\vec{k}|}$  is now reached only on the border of the integration region (see points  $A$  in Fig. 4) and therefore presents no problem for numerical integration. The dimension of the integral equation (2.12) can be further reduced by noting that only the  $\phi$ -integrated quantities

$$\sigma^{(0)}(p, \theta_p; k) = \int_0^{2\pi} \frac{d\phi_p}{2\pi} \sigma(\vec{p}, k) \quad (2.15)$$

and

$$K^{(0)}(p, \theta_p, p', \theta_{p'}) = \int_0^{2\pi} \frac{d(\phi_p - \phi_{p'})}{2\pi} K(\vec{p}, \vec{p}'; k) \quad (2.16)$$

are needed to calculate  $\Pi_N(k)$ . The actual proof that  $K^{(0)}$  does not depend on  $(\phi_p + \phi_{p'})/2$  is given in Appendix A. The self-energy is finally obtained in the form

$$\Pi_N(k) = 4k^2 \left( \frac{f_\pi \Gamma}{m_\pi} \right)^2 \cdot \int_{\mathcal{R}} \frac{dp p^2 d(\cos\theta_p)}{4\pi^2} \frac{\sigma^{(0)}(p, \theta_p; k)}{\epsilon_p - \epsilon_{|\vec{p}-\vec{k}|}} \quad (2.17)$$

and  $\sigma^{(0)}$  is determined from

$$\sigma^{(0)}(p, \theta_p; k) = 1 + \int_{\mathcal{R}} \frac{dp' p'^2 d(\cos\theta_{p'})}{4\pi^2} \frac{K^{(0)}(p, \theta_p, p', \theta_{p'}; k)}{\epsilon_{p'} - \epsilon_{|\vec{p}'-\vec{k}|}} \times \sigma^{(0)}(p', \theta_{p'}; k). \quad (2.18)$$

The integration region  $\mathcal{R}$  is given explicitly in Fig. 4.

#### B. Inclusion of $\Delta$ isobars

In this section, we will extend the formalism of Sec. II A to include the  $\Delta$  isobar in the calculation

of the static pion  $p$ -wave self-energy in symmetric nuclear matter. We treat the  $\Delta$  isobar as an elementary particle in the many-body system, which is justified according to Ref. 22. Note that the  $\Delta$  isobar has spin and isospin  $\frac{3}{2}$ . In addition to the diagram in Fig. 1, we now also have to calculate the diagrams in Fig. 6. We have to consider both diagrams because we can distinguish between a nucleon line and a  $\Delta$ -isobar line. After some manipulations analogous to those in Sec. II A, these terms are given in the static limit ( $\Omega = 0$ ) by

$$\Pi_{\Delta}(k, \Omega = 0) = \sum_{TSM_S} \int_F \frac{d^3p}{(2\pi)^3} \left[ \frac{\tau_{\Delta}^0(TSM_S k) \tau_{\Delta}^*(TSM_S; \vec{p} - \vec{k}/2, k)}{\epsilon_p - \epsilon_{|\vec{p}-\vec{k}|}^{\Delta} - \omega_{\Delta}} + \frac{\tau_{\Delta}^{0*}(TSM_S k) \tau_{\Delta}(TSM_S; U(\vec{p} - \vec{k}/2), k)}{\epsilon_p - \epsilon_{|\vec{p}-\vec{k}|}^{\Delta} - \omega_{\Delta}} \right], \quad (2.19)$$

where the first term in the integral corresponds to Fig. 6(a) and the second to Fig. 6(b). The integration extends over the whole Fermi sphere; the operation  $U$  is defined in Eq. (2.7); and the bare  $\pi N \Delta$  vertices  $\tau_{\Delta}^0$  and  $\tau_{\Delta}^{0*}$  are both given by

$$\begin{aligned} \tau_{\Delta}^0(TSM_S k) &= \tau_{\Delta}^{0*}(TSM_S k) \\ &= \frac{f_{\pi}^* \Gamma_{\Delta}(k)}{m_{\pi}} \frac{4}{3} k \delta_{T,1} \delta_{S,1} \delta_{M_S,0}. \end{aligned} \quad (2.20)$$

They can be calculated analogous to Eq. (2.2) by simply replacing one of the spin-isospin  $\frac{1}{2}$  states by a  $\frac{3}{2}$  state and using the spin-isospin transition operators  $\vec{S}, T_z$  and  $\vec{S}^*, T_z^*$  for  $\tau_{\Delta}^0$  and  $\tau_{\Delta}^{0*}$ , respectively, instead of  $\vec{\sigma}$  and  $\tau_z$ . In Eq. (2.20)  $f_{\pi}^*$  is the  $\pi N \Delta$  coupling constant and  $\Gamma_{\Delta}(k)$  is the form factor for this vertex; the actual values used in the calculation are given in Table II of Appendix A. The

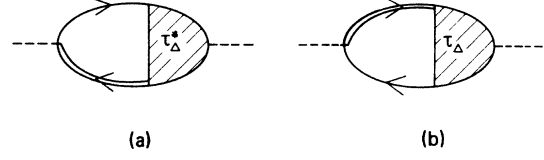


FIG. 6. Contribution to the pion self-energy when  $\Delta$  isobars are included. Note that diagrams (a) and (b) have different time structure.

energy denominators in  $\Pi_{\Delta}$  contain the nucleon s.p. energy  $\epsilon_p$ , the  $\Delta$ -isobar s.p. energy  $\epsilon_{|\vec{p}-\vec{k}|}^{\Delta}$ , and  $\omega_{\Delta}$ , the mass difference between a  $\Delta$  isobar and a nucleon. To calculate the dressed vertices  $\tau_{\Delta}^*$  and  $\tau_{\Delta}$ , we have to take into account the coupling between nucleon particle-hole states and  $\Delta$ -isobar hole states. Therefore these vertices will couple to the nucleon vertex  $\tau$ , discussed in Sec. II A, which we will denote in the following  $\tau_N$ . In Fig. 7 this is shown in terms of diagrams. The interaction blocks are again irreducible with respect to vertical ph,  $\Delta h$ , and one-pion cuts. The interaction block joining nucleon ph states is the same as discussed in Sec. II A but will be denoted by  $\tilde{G}_N$  in the following (see also Sec. III A). The transition from ph to  $\Delta h$  states is represented by  $\tilde{G}_{\Delta}$ ; it is discussed in Sec. III B. The interaction between  $\Delta h$  states has two constituents,  $\tilde{G}_{\Delta\Delta}^F$  and  $\tilde{G}_{\Delta\Delta}^B$ , representing forward and backward going diagrams

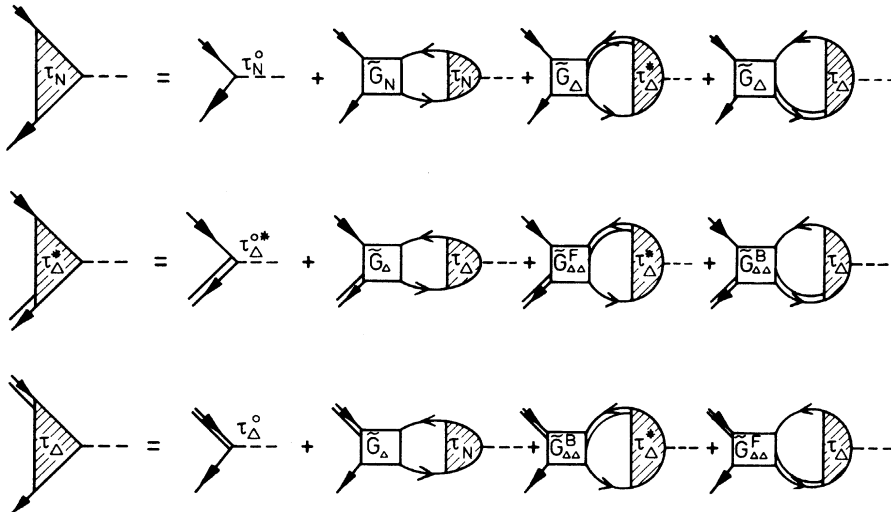


FIG. 7. Coupled set of integral equations for the dressed  $\pi NN$  and  $\pi N \Delta$  vertices [see Eq. (2.21)].

respectively. They are discussed in Sec. III C. Details of the ph transformations for these interactions can be found in Appendix A. These equations allow a coupling of the pion channel ( $S=1$ ,  $M_S=0$ ) to intermediate  $\Delta h$  states with  $S=1$ ,  $M_S=0$  and  $S=2$ ,  $M_S=\pm 2$  [see Appendix A, Eq. (A 20) and the discussion following this equation]. Numerically, however, the coupling to  $\Delta h$  states with  $S=2$ ,

$M_S=\pm 2$  was found to be negligible. Therefore we will suppress all spin isospin indices in the following, these quantum numbers being fixed at  $S=1$ ,  $M_S=0$ , and  $T=1$ . Treating the energy dependence of the  $\tilde{G}_N$  block as in Sec. II A and discarding any energy dependence in the other interaction blocks, we obtain the coupled integral equations displayed in Fig. 7 in the form (see Sec. II A)

$$\begin{aligned} \tau_N(\vec{p}; k) = & \tau_N^0(k) + \int_R \frac{d^3 p'}{(2\pi)^3} \frac{1}{\epsilon_{p'} - \epsilon_{|\vec{p}' - \vec{k}|}} [\tilde{G}_N(\vec{p}, \vec{p}' - \vec{k}/2; k) \tau_N(\vec{p}' - \vec{k}/2; k) + \tilde{G}_N(\vec{p}, U(\vec{p}' - \vec{k}/2); k) \tau_N(U(\vec{p}' - \vec{k}/2); k)] \\ & + \int_F \frac{d^3 p'}{(2\pi)^3} \frac{1}{\epsilon_{p'} - \epsilon_{|\vec{p}' - \vec{k}|} - \omega_\Delta} [\tilde{G}_\Delta(\vec{p}, \vec{p}' - \vec{k}/2; k) \tau_\Delta^*(\vec{p}' - \vec{k}/2; k) + \tilde{G}_\Delta(\vec{p}, U(\vec{p}' - \vec{k}/2); k) \tau_\Delta(U(\vec{p}' - \vec{k}/2); k)], \end{aligned} \quad (2.21a)$$

$$\begin{aligned} \tau_\Delta^*(\vec{p}; k) = & \tau_\Delta^{0*}(k) + \int_R \frac{d^3 p'}{(2\pi)^3} \frac{1}{\epsilon_{p'} - \epsilon_{|\vec{p}' - \vec{k}|}} [\tilde{G}_\Delta(\vec{p}, \vec{p}' - \vec{k}/2; k) \tau_N(\vec{p}' - \vec{k}/2; k) + \tilde{G}_\Delta(\vec{p}, U(\vec{p}' - \vec{k}/2); k) \tau_N(U(\vec{p}' - \vec{k}/2); k)] \\ & + \int_F \frac{d^3 p'}{(2\pi)^3} \frac{1}{\epsilon_{p'} - \epsilon_{|\vec{p}' - \vec{k}|} - \omega_\Delta} [\tilde{G}_{\Delta\Delta}^F(\vec{p}, \vec{p}' - \vec{k}/2; k) \tau_\Delta^*(\vec{p}' - \vec{k}/2; k) + \tilde{G}_{\Delta\Delta}^B(\vec{p}, U(\vec{p}' - \vec{k}/2); k) \tau_\Delta(U(\vec{p}' - \vec{k}/2); k)], \end{aligned} \quad (2.21b)$$

$$\begin{aligned} \tau_\Delta(\vec{p}, k) = & \tau_\Delta^0(k) + \int_R \frac{d^3 p'}{(2\pi)^3} \frac{1}{\epsilon_{p'} - \epsilon_{|\vec{p}' - \vec{k}|}} [\tilde{G}_\Delta(\vec{p}, \vec{p}' - \vec{k}/2; k) \tau_N(\vec{p}' - \vec{k}/2; k) + \tilde{G}_\Delta(\vec{p}, U(\vec{p}' - \vec{k}/2); k) \tau_N(U(\vec{p}' - \vec{k}/2); k)] \\ & + \int_F \frac{d^3 p'}{(2\pi)^3} \frac{1}{\epsilon_{p'} - \epsilon_{|\vec{p}' - \vec{k}|} - \omega_\Delta} [\tilde{G}_{\Delta\Delta}^B(\vec{p}, \vec{p}' - \vec{k}/2; k) \tau_\Delta^*(\vec{p}' - \vec{k}/2; k) + \tilde{G}_{\Delta\Delta}^F(\vec{p}, U(\vec{p}' - \vec{k}/2); k) \tau_\Delta(U(\vec{p}' - \vec{k}/2); k)]. \end{aligned} \quad (2.21c)$$

The integration area for nucleon ph states is again restricted to region  $R$  (see Fig. 4), whereas the  $\Delta h$  phase space ranges over the entire Fermi sphere. In addition to Eq. (2.11) we define

$$\sigma_\Delta(\vec{p}; k) = \frac{1}{2\tau_\Delta^0(k)} [\tau_\Delta^*(\vec{p} - \vec{k}/2; k) + \tau_\Delta(U(\vec{p} - \vec{k}/2); k)]. \quad (2.22)$$

Using the symmetry relation (A15), the integral equations reduce to

$$\sigma_N(\vec{p}; k) = 1 + \int_R \frac{d^3 p'}{(2\pi)^3} K_N(\vec{p}, \vec{p}'; k) \frac{1}{\epsilon_{p'} - \epsilon_{|\vec{p}' - \vec{k}|}} \sigma_N(\vec{p}'; k) + \alpha(k) \int_F \frac{d^3 p'}{(2\pi)^3} K_\Delta(\vec{p}, \vec{p}'; k) \frac{1}{\epsilon_{p'} - \epsilon_{|\vec{p}' - \vec{k}|} - \omega_\Delta} \sigma_\Delta(\vec{p}'; k), \quad (2.23a)$$

$$\sigma_\Delta(\vec{p}; k) = 1 + \frac{1}{\alpha(k)} \int_R \frac{d^3 p'}{(2\pi)^3} K_\Delta(\vec{p}, \vec{p}'; k) \frac{1}{\epsilon_{p'} - \epsilon_{|\vec{p}' - \vec{k}|}} \sigma_N(\vec{p}'; k) + \int_F \frac{d^3 p'}{(2\pi)^3} K_{\Delta\Delta}(\vec{p}, \vec{p}'; k) \frac{1}{\epsilon_{p'} - \epsilon_{|\vec{p}' - \vec{k}|} - \omega_\Delta} \sigma_\Delta(\vec{p}'; k), \quad (2.23b)$$

where  $K_n$  is defined in Eq. (2.13) and

$$K_\Delta(\vec{p}, \vec{p}'; k) = \tilde{G}_\Delta(\vec{p} - \vec{k}/2, \vec{p}' - \vec{k}/2; k) + \tilde{G}_\Delta(\vec{p} - \vec{k}/2, U(\vec{p}' - \vec{k}/2); k), \quad (2.24)$$

$$K_{\Delta\Delta}(\vec{p}, \vec{p}'; k) = \tilde{G}_{\Delta\Delta}^F(\vec{p} - \vec{k}/2, \vec{p}' - \vec{k}/2; k) + \tilde{G}_{\Delta\Delta}^B(\vec{p} - \vec{k}/2, U(\vec{p}' - \vec{k}/2); k), \quad (2.25)$$

and lastly

$$\alpha(k) = \frac{\tau_\Delta^0(k)}{\tau_N^0(k)} = \frac{2f_\pi^* \Gamma_\Delta(k)}{3f_\pi \Gamma_N(k)}. \quad (2.26)$$

The dimension of the integral equations can be further reduced by eliminating the  $\phi$  dependence as in Sec. II A. The final equations which are solved numerically are

$$\begin{aligned} \sigma_N^{(0)}(p, \theta_p; k) = & 1 + \int_R \frac{dp' p'^2 d(\cos\theta_{p'})}{4\pi^2} \frac{K_N^{(0)}(p\theta_p, p'\theta_{p'}; k)}{\epsilon_{p'} - \epsilon_{|\vec{p}' - \vec{k}|}} \sigma_N^{(0)}(p', \theta_{p'}; k) \\ & + \alpha(k) \int_F \frac{dp' p'^2 d(\cos\theta_{p'})}{4\pi^2} \frac{K_{\Delta\Delta}^{(0)}(p\theta_p, p'\theta_{p'}; k)}{\epsilon_{p'} - \epsilon_{|\vec{p}' - \vec{k}|} - \omega_\Delta} \sigma_\Delta^{(0)}(p', \theta_{p'}; k), \end{aligned} \quad (2.27a)$$

$$\begin{aligned} \sigma_{\Delta}^{(0)}(p, \theta_p; k) = & 1 + \frac{1}{\alpha(k)} \int_R \frac{dp' p'^2 d(\cos\theta_{p'})}{4\pi^2} \frac{K_{\Delta}^{(0)}(p\theta_p, p'\theta_{p'}; k)}{\epsilon_{p'} - \epsilon_{|p-\vec{p}'-k|}} \sigma_N^{(0)}(p', \theta_{p'}; k) \\ & + \int_F \frac{dp' p'^2 d(\cos\theta_{p'})}{4\pi^2} \frac{K_{\Delta\Delta}^{(0)}(p\theta_p, p'\theta_{p'}; k)}{\epsilon_{p'} - \epsilon_{|p-\vec{p}'-k|} - \omega_{\Delta}} \sigma_{\Delta}^{(0)}(p', \theta_{p'}; k), \end{aligned} \quad (2.27b)$$

where the  $\phi$ -integrated quantities are defined as in Sec. II A. The solutions  $\sigma_N^{(0)}(p, \theta_p; k)$  and  $\sigma_{\Delta}^{(0)}(p, \theta_p; k)$  are then used to calculate the total pion self-energy

$$\begin{aligned} \Pi(k) = \Pi_N(k) + \Pi_{\Delta}(k) = & 4k^2 \left[ \frac{f_{\pi} \Gamma_N(k)}{m_{\pi}} \right]^2 \int_R \frac{dp p^2 d(\cos\theta_p)}{4\pi^2} \frac{\sigma_N^{(0)}(p, \theta_p; k)}{\epsilon_p - \epsilon_{|p-\vec{k}|}} \\ & + \frac{16}{9} k^2 \left[ \frac{f_{\pi} \Gamma_{\Delta}(k)}{m_{\pi}} \right]^2 \int_F \frac{dp p^2 d(\cos\theta_p)}{4\pi^2} \frac{\sigma_{\Delta}^{(0)}(p, \theta_p; k)}{\epsilon_p - \epsilon_{|p-\vec{k}|} - \omega_{\Delta}}. \end{aligned} \quad (2.28)$$

### III. DISCUSSION OF THE INTERACTIONS

#### A. Nucleon-nucleon ph interaction

Our approximation to the irreducible ph-interaction block will be a Brueckner  $G$  matrix with direct static one-pion-exchange (OPE) subtracted. We have used two different bare interactions as input for the  $G$ -matrix calculation. One is the Reid soft-core potential<sup>19</sup> supplemented in higher partial waves ( $J > 2$ ) by an OBE potential. The other is one of the Bonn potentials, the so-called  $HM2 + \Delta(550)$ .<sup>20</sup> Both potentials are realistic in the sense that they describe the  $NN$  data. The Bonn potential, however, has a weaker tensor force. Nevertheless, in a lowest order Brueckner calculation it yields saturation properties which are similar to those for the Reid potential. Therefore it is interesting to see whether any significant differences show up in a calculation of the pion self-energy. To obtain the  $G$  matrix for nuclear matter, the Bethe-Goldstone equation has been solved in momentum space using the matrix inversion technique as it is described in Ref. 23.

For the hole energies the effective mass approximation is used:

$$\epsilon(k) = \frac{k^2}{2m_B^*} - V_0, \quad (3.1)$$

where the constants  $m_B^*$  and  $V_0$  are determined self-consistently. Kinetic energies were used for the particle spectrum, the so-called "standard" choice. Since our calculation of the pion self-energy is sensitive to ph-excitation energies, we will use a more physical single particle spectrum by taking a continuous choice across the Fermi surface for this calculation. First we have considered the  $m^*$  approximation (Landau choice) for the whole spectrum,

$$\epsilon(k) = \frac{k^2}{2m_L^*} - V_L.$$

This is used in all calculations of the pion self-energy. As a prescription for the effective mass for a specific force at a specific density we have used the Landau effective mass calculated for this specific  $G$  matrix. It is worth noting that the Landau effective mass  $m_L^*$  agrees quite closely in each case with the Brueckner effective mass  $m_B^*$  defined in (3.1). Another continuous choice for the single particle spectrum we have used is to approximate the calculated Brueckner energy for holes,

$$\epsilon(k) = \frac{k^2}{2M} + \sum_{k' < k_F} \langle kk' | G(\epsilon(k) + \epsilon(k')) | kk' \rangle, \quad k < k_F \quad (3.2)$$

and the particle energies by a power series in  $k$  up to  $k^5$ , with the restrictions that this series closely reproduces (3.2) below  $k_F$ ; at  $k_F$  the energy and its derivative with respect to  $k$  are continuous, and for  $k \geq 2.5k_F$  the energy becomes purely kinetic. In the following we will call this a "Brueckner spectrum."

The particle-particle  $G$ -matrix elements are calculated in momentum space using the  $LSJ$  representation. The starting energy has been chosen as discussed in Sec. II A and Appendix B [see Eq. (2.10)]. For each  $LSJ$  channel, or more precisely due to the tensor part of the interaction  $LL'SJ$  channel, the  $G$  matrix can be represented as a three dimensional array depending on initial and final relative momentum and the total c.m. momentum of the particle-particle states. The transformation to the particle-hole representation is discussed in Appendix A. Numerically it involves some angular momentum algebra and a three dimensional interpolation. The matrix elements for the mesh points of the momentum variables of the particle-hole (ph) representation have to be calculated from the three particle-particle momenta. In calculating the ph-matrix elements, particle-particle  $LSJ$  channels were considered up to  $J = 4$ . The higher partial waves are dominated

by one pion exchange (OPE). Since we have to subtract the direct piece anyhow, we have subtracted the Born approximation of OPE in  $LSJ$  representation from the  $G$  matrix up to  $J=4$  and have added the exchange piece of OPE separately in plane wave  $ph$  ( $SM_S T$ ) representation.<sup>24</sup> There is some ambiguity in this subtraction of OPE because the bare interactions contain OPE with some form factor. Since the Reid potential is only defined phenomenologically, this form factor is not defined. For the  $HM2+\Delta$ , the form factor is eikonal defined in terms of Mandelstam variables for the free nucleon-nucleon scattering. In view of this we have decided to neglect the form factor here, slightly overestimating the repulsion in the interaction only for very high pion momenta.

To get some feeling for the interactions which are used we list in Table I the Landau parameters which are appropriate for the pion channel. The general form of the Landau interaction is ( $|\vec{p}_1| = |\vec{p}_2| = k_F$ )

$$F_{\text{Landau}}(\vec{p}_1, \vec{p}_2) = f(\vec{p}_1, \vec{p}_2) + f'(\vec{p}_1, \vec{p}_2) \vec{\tau}_1 \cdot \vec{\tau}_2 \\ + [g(\vec{p}_1, \vec{p}_2) + g'(\vec{p}_1, \vec{p}_2) \vec{\tau}_1 \cdot \vec{\tau}_2] \vec{\sigma}_1 \cdot \vec{\sigma}_2 \\ + [h(\vec{p}_1, \vec{p}_2) + h'(\vec{p}_1, \vec{p}_2) \vec{\tau}_1 \cdot \vec{\tau}_2] (q/k_F)^2 S_{12}(\vec{q}), \quad (3.3)$$

where  $\vec{\sigma}$  and  $\vec{\tau}$  denote Pauli spin and isospin matrices, respectively. The tensor operator is defined by

$$S_{12}(\vec{q}) = (3\vec{\sigma}_1 \cdot \vec{q} \vec{\sigma}_2 \cdot \vec{q} - \vec{\sigma}_1 \cdot \vec{\sigma}_2 q^2) / q^2 \quad (3.4)$$

and  $\vec{q} = \frac{1}{2}(\vec{p}_1 - \vec{p}_2)$ . The functions  $f$ ,  $f'$ ,  $g$ , etc. of Eq. (3.3) depend only on the angle between  $\vec{p}_1$  and

$\vec{p}_2$  and therefore can be expanded in Legendre polynomials like, e.g.,

$$N_0 f(\vec{p}_1, \vec{p}_2) = \sum_l F_l P_l(\cos\theta).$$

To get the dimensionless numbers  $F_l$ ,  $F'_l$ ,  $G_l$ , etc., which are called Landau parameters, one multiplies the functions  $f$ ,  $f'$ ,  $g$ , etc. with the density of states  $N_0$  at the Fermi surface

$$N_0 = \frac{2k_F m^*}{\pi^2}.$$

The density of states contains the Landau effective mass  $m^*$  which is calculated from the Landau parameter  $F_1$  by

$$\frac{m^*}{m} = 1 + \frac{1}{3} F_1.$$

Note that these parameters apply strictly to the limiting case of the  $ph$  momentum, which in the calculation of pion self-energies is equal to the pion momentum, going to zero.

Since we treat the energy dependence of the  $G$  matrix in our calculation of the pion self-energy, we include in brackets the values of some parameters calculated for a starting energy defined by Eq. (B5). Mainly the  $G'_0$  parameter is affected, being effectively somewhat smaller. The tensor parameters are unaffected. At this stage it is also useful to define another measure of an interaction strength in the pion channel. We define an interaction strength  $\gamma_N$  for an interaction of the form  $\gamma_N \vec{\sigma}_1 \cdot \vec{\sigma}_2 \vec{\tau}_1 \cdot \vec{\tau}_2$  (central interaction) to have the value

TABLE I. Landau parameters for the interactions Reid and  $HM2+\Delta$ , at the two densities at which our calculations are performed. In the Bethe-Goldstone equation a starting energy  $W = -10$  MeV has been used. The numbers in parentheses are calculated for a starting energy which has been chosen according to Eq. (B5). The parameters are normalized by multiplying with the density of states  $N_0 = 2k_F m^* / \pi^2$ .

	Reid		$HM2+\Delta$	
	$k_F = 1.40$	$k_F = 1.77$	$k_F = 1.40$	$k_F = 1.77$
$m^*/m$	0.60 (0.60)	0.52 (0.52)	0.62 (0.62)	0.55 (0.55)
$G'_0$	0.81 (0.75)	0.84 (0.79)	0.74 (0.70)	0.72 (0.69)
$G'_1$	0.02 (-0.01)	-0.06 (-0.09)	0.18 (0.15)	0.20 (0.19)
$G_2$	0.05	0.01	0.03	0.07
$G_3$	0.04	0.05	-0.01	0.01
$H'_0$	-0.60	-0.77	-0.63	-0.79
$H'_1$	-0.87	-1.17	-0.94	-1.32
$H'_2$	-0.81	-1.22	-0.81	-1.29
$H'_3$	-0.61	-1.06	-0.60	-1.08
$H'_4$	-0.44	-0.86	-0.42	-0.84

$-\frac{1}{3}$  for the  $\delta$ -function piece of direct static OPE. For example the Landau parameter  $G'_0$  for the Reid potential at  $k_F = 1.4 \text{ fm}^{-1}$  gives a strength of 0.48 according to the conversion

$$\gamma_N = \frac{m_\pi^2}{f_\pi^2} \frac{\pi^2}{2m^*k_F} G'_0. \quad (3.5)$$

### B. $\Delta$ -isobar nucleon-hole ph interaction

This interaction provides the coupling between nucleon ph and  $\Delta$ h states. When only one meson is exchanged in this transition, this meson must have at least isospin one since at one vertex a nucleon ( $t = \frac{1}{2}$ ) is converted into a  $\Delta$  isobar ( $t = \frac{3}{2}$ ). Therefore we will consider  $\pi$  and  $\rho$  exchange for this bare transition potential. We will use  $\pi$ - and  $\rho$ -range propagators [ $1/(m_\pi^2 + k^2)$ ] in the transition potential although this tends to overestimate the strength<sup>25</sup> since energy transfer reduces the matrix elements. The main reason for this choice is that in summing the diagrams for the pion propagator [Eq. (1.1)] one usually considers only free pion propagation in intermediate states; however, as soon as intermediate  $\Delta$  isobars appear in the self-energy diagram the same problem of an overestimate arises. Therefore to be consistent in this respect we have chosen for nonrelativistic static  $\pi$ - and  $\rho$ -range transition potentials.

There are of course other processes which can contribute to this interaction. Especially the treatment of short-range correlations seems to be important. Instead of solving a coupled set of Bethe-Goldstone equations, we have taken into account the effects of correlations between nucleons by calculating an effective transition potential

$$G_\Delta = \left(1 + G_N \frac{Q}{e}\right) V_\Delta, \quad (3.6)$$

where  $G_N$  is the nucleon  $G$  matrix,  $Q$  is the Pauli operator,  $e$  the propagator for intermediate nucleons and  $V_\Delta$  the bare transition potential. To obtain the irreducible interaction block  $\tilde{G}_\Delta$ , direct OPE has to be subtracted and a particle-hole transformation must be performed (see Appendix A).

To calculate  $G_\Delta$  in the particle-particle direction one simply takes a nucleon-nucleon correlation function in a specific  $LSJ$  channel, matches this with an  $LSJ$  channel of the bare transition potential, and integrates over intermediate relative momenta. Because we consider an  $NN$  to  $N\Delta$  transition, the isospin must be one. This means that the most important contribution is expected to come from the  $^1S_0$  correlation function. Due to angular momentum and parity conservation, however, the only transition channel is the  $^1S_0$ - $^5D_0$

(see Fig. 8). This is a pure tensor transition which tends to be of relatively long range, the short range  $\rho$  exchange canceling the short range piece of  $\pi$  exchange. Numerically this means that for the second term of Eq. (3.6) one gets a negligible contribution because the  $^1S_0$  correlation function and the longer ranged, purely tensor transition amplitude peak at different relative momenta. This means that the contribution from correlation effects is very small for  $NN$  to  $N\Delta$  transitions.

There is, however, another source of repulsion in this channel which is rather large and originates from the bare transition potential. To make this clear, consider the central part of the relevant ph matrix element ( $S=1$ ,  $T=1$ ) for the bare  $\pi$ -exchange transition potential [see Eq. (A.28)],

$$\langle \vec{k}, \vec{p}_1 | V_{N\Delta}^\pi | \vec{k}, \vec{p}_2 \rangle = -\frac{f_\pi f_\pi^*}{m_\pi^2} \left[ \frac{8}{9} \frac{k^2}{m_\pi^2 + k^2} - \frac{8}{9} \frac{(\vec{p}_1 - \vec{p}_2)^2}{m_\pi^2 + (\vec{p}_1 - \vec{p}_2)^2} \right], \quad (3.7)$$

where  $\vec{k}$  is the total ph momentum,  $\vec{p}_1$  and  $\vec{p}_2$  initial and final relative momentum, and  $f_\pi, f_\pi^*$  the coupling constants discarding form factors for simplicity. The first term is the direct piece which has to be subtracted. Note, however, that the second part, the exchange piece, is strongly repulsive. In fact, if we define an interaction strength  $\gamma_\Delta$  for the  $\delta$  function of the direct piece to be  $-\frac{1}{3}$  analogous to the  $NN$  case [see Eq. (3.5)], we see that the  $\delta$  function of the exchange piece has  $\gamma_\Delta$

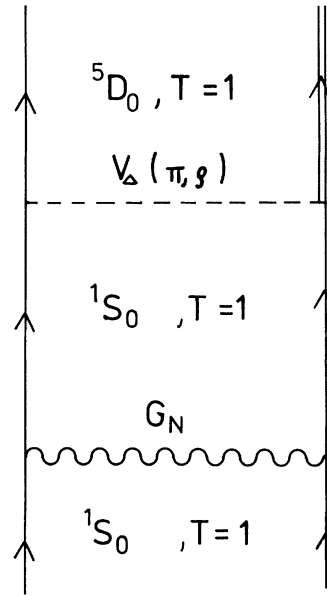


FIG. 8. Only contribution to the  $NN$ - $N\Delta$  transition potential (3.6) where  $NN$  correlations could be important. It almost vanishes, however, due to momentum mismatch.

$= +\frac{1}{3}$ . The factor  $\frac{8}{3}$  in Eq. (3.7) is due to spin isospin coupling. To understand how this  $\delta$ -function part contributes in spite of  $NN$  correlations, we have to consider diagrams for the *total* pion propagator. Consider part of a diagram where a pion propagates from a  $ph$  to a  $\Delta h$  state. There is, of course, also an exchange diagram (see Fig. 9). The sum of the diagrams 9 is zero in the antisymmetrized particle-particle channel for an  $L=0$  to  $L'=0$  transition due to the  $S=1, T=1$  nature of the interaction. In the calculation of the self-energy of the pion, diagram 9(a) is reducible and has to be subtracted. Thus one gets a contribution from one pion exchange in a  $T=1, {}^3S_1$  particle-particle channel. In such an  $L=0$  to  $L'=0$  transition one gets a contribution from the  $\delta$ -function part of the one pion exchange. A similar consideration about the presence of the  $\delta$ -function part of the OPE is also valid for the  ${}^3S_1$  and  ${}^1S_0$   $NN$  interaction. In the  $NN$  case, however, the exchange part is by a factor of 4 smaller than the direct part. In addition to this repulsive  $\delta$ -function term, more repulsion comes from the exchange contribution of  $\rho$  exchange. The direct part of  $\rho$  exchange does not contribute since it is not compatible with pion quantum numbers. Therefore there is repulsion in this transition channel which is not due to short range correlations.

### C. $\Delta$ -isobar-hole $\Delta$ -isobar-hole interaction

In this subsection we will discuss the contributions to this interaction from the particle-particle direction. Then we can distinguish between two types of contributions, the first has a  $\Delta$  isobar in the initial and final state contributing to  $\tilde{G}_{\Delta\Delta}^F$ ; this means that after  $ph$  transformation these processes are so-called "forward going" [see Figs. 10(a) and 10(b)] because the  $\Delta$  isobar cannot be a hole. The other type has two  $\Delta$  isobars in the initial or final state and gives "backward going" diagrams contributing to  $\tilde{G}_{\Delta\Delta}^B$  after  $ph$  transformation [see Fig. 10(c)].

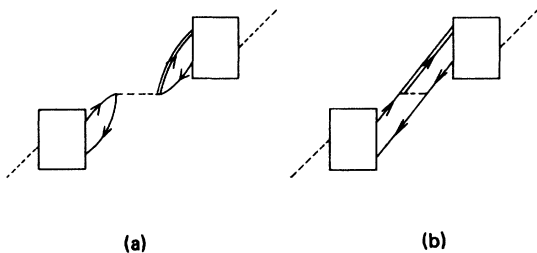


FIG. 9. Two diagrams that contribute to the total pion propagator. The boxes in diagrams (a) and (b) are the same, representing any process which connects the parts of the diagrams explicitly shown.

We will first discuss the processes in Figs. 10(a) and 10(b). Two cases can be considered, sometimes referred to as direct (b) and exchange (a) terms. The simplest contribution to direct processes is again the bare transition potential. There is, however, the problem that such transition potentials contain one  $\Delta\Delta$ -meson vertex on which there is very little knowledge. In a one-boson-exchange picture any meson that contributes in the  $NN$  case contributes here, too. But whereas for example the  $\sigma$  meson is constrained by a fit to  $NN$  data, no such restrictions are present here. In view of these uncertainties and also because the contribution from Fig. 10(b) turned out to be small if only  $\pi$  and  $\rho$  exchange are considered, we have chosen to set all  $\Delta\Delta$ -meson vertices equal to zero. As a consequence of this the leading term of the  $\Delta$  self-energy is zero, and therefore we will neglect any self-energy contribution to the  $\Delta$  propagator, which means that the  $\Delta$  isobar s.p. spectrum is pure kinetic energy. Since both effects work in opposite directions, inclusion of  $\Delta\Delta$ -meson vertices would make the  $\Delta h$ - $\Delta h$  interaction more repulsive, working against pion condensation; a single particle spectrum for the  $\Delta$  isobar similar to that for a nucleon, on the other hand, would make the  $\Delta h$  energy denominator smaller, favoring condensation; we believe that quantitatively our procedure does not lead to large uncertainties in the final results. For diagram 10(a) we consider  $\pi$  and  $\rho$  exchange multiplied with a correlation function. Since the correlation function corresponding to Fig. 10(a) is not known, we make the minimal assumption that the  $\delta$ -function pieces of the interaction are suppressed by the

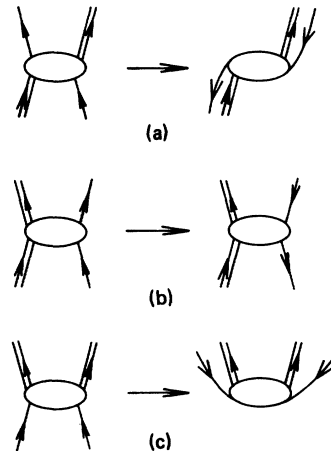


FIG. 10. Diagrams (a) and (b) show the different contributions to forward going diagrams while (c) gives the contribution to backward going diagrams. The  $ph$  transformations are shown explicitly.

correlation function.<sup>11</sup> If we now subtract the reducible one-pion exchange, and keep in mind that the total one-rho exchange does not contribute since it has the wrong quantum numbers, only the subtracted  $\delta$ -function pieces remain.

Now we come to the second type of contribution to the  $\Delta h$ - $\Delta h$  interaction [Fig. 10(c)]. Again we have the bare  $\pi$ - and  $\rho$ -exchange long range transition potentials, but in addition we include the effects of short range nucleon-nucleon correlations by defining an effective transition potential analogous to Sec. IIIB,

$$G_{\Delta\Delta} = V_{\Delta\Delta} + G_N \frac{Q}{e} V_{\Delta\Delta}, \quad (3.8)$$

where  $G_N$ ,  $Q$ , and  $e$  have the same meaning as in Eq. (3.6) and  $V_{\Delta\Delta}$  is the bare transition potential. To obtain the contribution to the irreducible interaction block  $\bar{G}_{\Delta\Delta}^B$  direct OPE has to be subtracted and a ph transformation must be performed (see Appendix A). The second part of Eq. (3.7) now has two contributions from S-wave correlation functions (both  $^1S_0$  and  $^3S_1$ ). In addition both S-wave transition amplitudes are possible. Therefore, in this case there is a non-negligible contribution from short range correlations. Numerically this contribution is almost independent of the momenta involved, at least in the relevant region defined by the integration interval of the integral equation for all considered total momenta. The reason is that the correlation functions are not sensitive to initial relative momenta, and, on the other hand, the transition amplitude is very flat so that upon integrating over intermediate relative momenta the result is not very sensitive to initial and final relative momentum. This is valid for both S-wave contributions, which are in fact almost equal. Since there is not more than 5% variation in these matrix elements we have represented this contribution by a constant interaction strength. If we define an interaction strength  $\gamma_{\Delta\Delta}$  for this interaction analogous to  $\gamma_N$  and  $\gamma_\Delta$ , we find this contribution to have  $\gamma_{\Delta\Delta} = 0.25$ .

#### IV. RESULTS AND DISCUSSION

##### A. Nucleons only

The calculations have been performed for two densities, the first being approximately the empirical saturation density  $k_F = 1.40 \text{ fm}^{-1}$  and the other being  $k_F = 1.77 \text{ fm}^{-1}$  which corresponds to approximately twice this saturation density. First we will discuss the results when only nucleon particle-hole states are considered. In Fig. 11 the results are displayed for  $k_F = 1.40 \text{ fm}^{-1} = 276.2 \text{ MeV}/c$ . Here we do not plot the self-energy but the inverse of the pion propagator (at  $\omega = 0$  and

with an extra minus sign) as a function of the pion momentum  $k$ . In this plot pion condensation would occur, according to Eq. (1.1), when the inverse of the propagator crosses zero; this defines the critical momentum at the same time. It should be recalled that in the present work the pion self-energy is calculated in the static limit only. Therefore the results for the inverse pion propagator displayed in this figure have a physical meaning only if the curve reaches the critical point. For reference, also the inverse of the free pion propagator is plotted. Two curves are drawn for the Reid potential, the difference being the choice of the single particle spectrum. Since there is hardly any difference in the interesting region  $K_F \sim k_F$  between the two curves, we will in the following only discuss results which are obtained with an  $m^*$  spectrum. Also plotted in Fig. 11 is the result for the  $HM2 + \Delta$  interaction. We conclude that this way of plotting the results does not distinguish between the two interactions at this density, which is below the threshold density for pion condensation.

Since it is one of the central aims of this investigation to study the role of the interaction, we

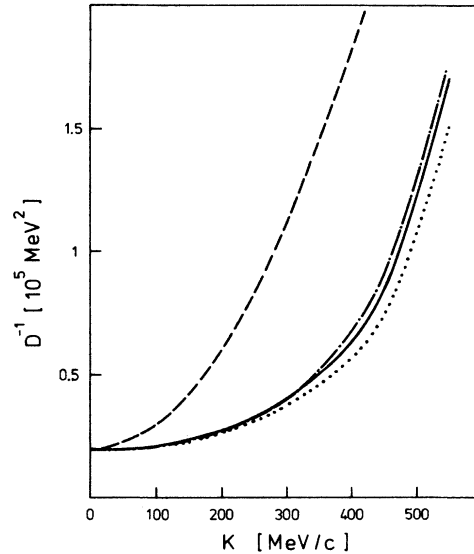


FIG. 11. The inverse of the static pion propagator  $D$  [see Eq. (1.1) with  $\omega = 0$ ] as a function of the momentum of the pion field. The dashed curve displays the free propagator  $D_0^{-1}$ . The dashed-dot and the solid curves are obtained calculating the pion self-energy  $\Pi$  for a Fermi momentum  $k_F = 1.4 \text{ fm}^{-1} = 276.2 \text{ MeV}/c$  using the  $NN$  potentials  $HM2 + \Delta$  and Reid soft core potentials, respectively. While for these two calculations the single particle spectrum is characterized by the Landau effective mass  $m^*$  only ( $\epsilon = k^2/2m^*$ ) a "Brueckner spectrum" and the Reid potential were used to obtain the dotted curve.

have analyzed our results in a simple model. If one assumes that for a given pion momentum  $k$  the interaction  $\bar{G}$  can be represented by  $\gamma_N(k)\vec{\sigma}_1 \cdot \vec{\sigma}_2 \vec{\tau}_1 \cdot \vec{\tau}_2$ , and if one uses an  $m^*$  spectrum, then the pion self-energy can be calculated analytically with the result

$$\Pi_N(k, \Omega = 0) = \frac{\Pi_N^{(0)}(k, \Omega = 0)}{1 - \gamma_N(k)\Pi_N^{(0)}/k^2}, \quad (4.1)$$

where  $\Pi_N^{(0)}$  is the pion self-energy due to nucleons without ph interactions.

$$\Pi_N^{(0)}(k, \Omega = 0) = -\left(\frac{f_1}{m}\right)^2 4k^2 \Gamma_N^2(k) \frac{m^* k_F}{2\pi^2} \phi_N(k/2k_F). \quad (4.2)$$

Here  $\phi_N$  is the Lindhard function in the static limit

$$\phi_N(\kappa) = \frac{1}{2} \left[ 1 - \frac{(1 - \kappa^2)}{2\kappa} \ln \left| \frac{1 - \kappa}{1 + \kappa} \right| \right]. \quad (4.3)$$

Now for each pion momentum  $k$  one can determine an effective strength  $\gamma_N(k)$  such that Eq. (4.1) gives the same result as the calculation using the full interaction  $\bar{G}$  of Eq. (2.5). Applying this model, one neglects the dependence on the relative ph momenta. This analysis only determines an average strength of the full interaction  $\bar{G}$  in the pion channel, which, for example, also contains a tensor component that cannot even be represented by  $\vec{\sigma}_1 \cdot \vec{\sigma}_2 \vec{\tau}_1 \cdot \vec{\tau}_2$ . Results of this analysis are given in Fig. 12 where the extracted  $\gamma_N$  is plotted as a

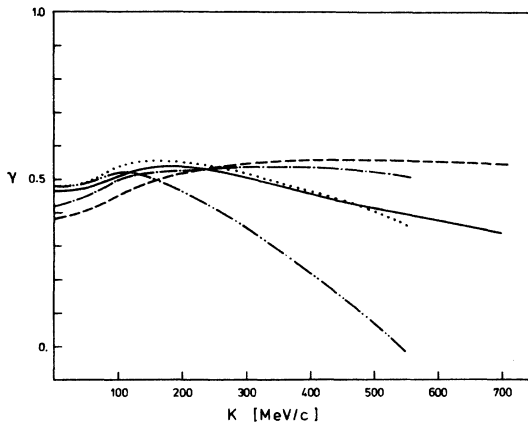


FIG. 12. Effective interaction strengths in the pion channel as defined in Eq. (4.1). The strengths are deduced from the calculation of pion self-energies for two different Fermi momenta and two different  $NN$  potentials. They are represented by a solid curve ( $k_F = 1.77 \text{ fm}^{-1}$ , Reid), a dotted curve ( $1.4 \text{ fm}^{-1}$ , Reid), a dashed curve ( $1.77 \text{ fm}^{-1}$ ,  $HM2 + \Delta$ ), and a dashed-dotted curve ( $1.4 \text{ fm}^{-1}$ ,  $HM2 + \Delta$ ). The dashed-dotted-dotted curve is obtained if only the central part of the Reid potential ( $k_F = 1.4 \text{ fm}^{-1}$ ) is considered. The relation between  $\gamma$  and the Landau parameter  $G'_0$  is given by Eq. (3.5).

function of the pion momentum for both densities and for both forces. These results show that for  $k_F = 1.4 \text{ fm}^{-1}$  there is hardly any difference between the Reid and the  $HM2 + \Delta$  in the critical region  $k \sim k_F$ , whereas for  $k_F = 1.77 \text{ fm}^{-1}$  the  $HM2 + \Delta$  is slightly more repulsive. However, taken as a function of the pion momentum, the curves of both forces show opposite behavior and only cross more or less in the critical region for both densities.

At small momenta there is in all four cases a characteristic increase; furthermore, all four curves approach, in the limit pion momentum to zero, the Landau limit  $G'_0$  [when  $\gamma_N$  is converted into  $G'_0$  following Eq. (3.5)]. Note that this limit is not the  $G'_0$  calculated from the  $G$  matrix with starting energy  $2\epsilon_F$ , but for a starting energy  $E_0$  according to Eq. (B5). Since in all four cases the latter is somewhat smaller, this can be interpreted as a weakening of the interaction because it has to simulate the contribution from diagrams with time overlapping  $G$  matrices as discussed in Sec. II A. We note that the phase space for this contribution is largest in the limit  $k$  to zero and decreases monotonically with  $k$  (see Sec. II A). Another interesting conclusion can be drawn from the limit of the curves for  $k$  to zero. It seems that here the contribution from the Landau tensor parameters somehow averages out although individually they are rather large (see Table I). To see how in general the curves are built up from central and tensor components, we have performed calculations where the interactions were averaged over the spin projections in the  $S=1$ ,  $T=1$  ph channel thereby obtaining the central part of the interaction. Since the result in all cases is rather similar we only show the result for the Reid potential at  $k_F = 1.40 \text{ fm}^{-1}$  as the dashed-dotted-dotted curve in Fig. 12. Indeed we see again the Landau limit for  $k$  to zero, but as  $k$  increases the contribution from the central part starts to fall off more and more rapidly. The conclusion therefore is that an important part of the repulsion in the pion channel is due to a tensor component which does not originate from direct single pion exchange because this is properly subtracted [see Eq. (2.5)]. This tensor component is increasingly important for increasing momenta.

#### B. Inclusion of $\Delta$ isobars

Since it is clear from Fig. 11 that both forces give similar results, we will now only discuss results for the Reid potential with inclusion of  $\Delta$  isobars. We see that inclusion of isobars does not lead to pion condensation at normal nuclear matter density. However, from Fig. 13 it is clear that at  $k_F = 1.77 \text{ fm}^{-1}$  inclusion of isobars establishes pion

condensation. In this figure we have also plotted a curve where we only took into account the result for  $\Pi_N$  [see Eq. (2.28)]. If we compare this curve with the result for nucleons only with the same force (Reid), which is also plotted, we see that inclusion of  $\Delta$ h intermediate states here leads to extra repulsion for  $\Pi_N$ . This also demonstrates that there is a considerable influence of  $\Delta$ h states on nucleon ph states in the pion channel. The additional term  $\Pi_\Delta$  in Eq. (2.28), which describes the contribution from the direct coupling of the pion to the  $\Delta$ h states, is rather attractive. At the density considered in Fig. 13 the inclusion of this isobar term even yields a phase transition to a pion condensate at values of the pion momentum roughly around  $k = k_F$ .

Since we do not learn very much about the interactions by looking at Figs. 11 and 13, we have analyzed the results again in a simple model. Assuming as in Sec. IV A constant interaction strengths, one can solve the coupled integral equations (2.21) analytically which then yields for the total pion self-energy  $\Pi = \Pi_N + \Pi_\Delta$  the following contributions:

$$\Pi_N(k) = \Pi_N^{(0)}(k)[1 + (\gamma_\Delta - \gamma_{\Delta\Delta})\Pi_\Delta^{(0)}(k)/k^2]/E \quad (4.4)$$

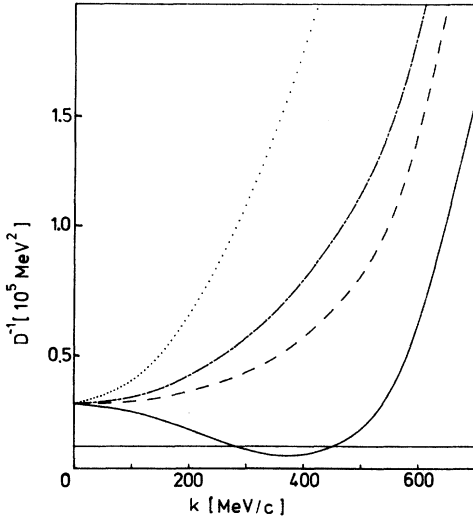


FIG. 13. The inverse of the static pion propagator  $D$  [see Eq. (1.1) with  $\omega = 0$ ] as a function of the momentum of the pion field at a Fermi momentum  $k_F = 1.77 \text{ fm}^{-1} = 349.2 \text{ MeV}/c$ . The Reid soft core potential has been used for the  $NN$  interaction. The full curve represents results for the total self-energy with inclusion of isobars, whereas the dashed-dotted curve gives the result if only contributions displayed in Fig. 1 are considered calculating the dressed vertex with inclusion of isobars [see also Eq. (4.4)]. For a reference this figure also contains the results  $D_0^{-1}$  for the free pion (dotted curve) and if the isobar contributions in calculating  $\Pi$  are at all neglected (dashed curve).

and

$$\Pi_\Delta(k) = \Pi_\Delta^{(0)}(k)[1 + (\gamma_\Delta - \gamma_N)\Pi_N^{(0)}(k)/k^2]/E, \quad (4.5)$$

where

$$E = 1 - \gamma_N \Pi_N^{(0)}(k)/k^2 - \gamma_{\Delta\Delta} \Pi_\Delta^{(0)}/k^2 + (\gamma_N \gamma_{\Delta\Delta} - \gamma_\Delta^2) \Pi_N^{(0)}(k) \Pi_\Delta^{(0)}(k)/k^4. \quad (4.6)$$

The interaction strengths were defined in Sec. III,  $\Pi_N^{(0)}$  is given in Eq. (4.2), and  $\Pi_\Delta^{(0)}$  which represents the pion self-energy due to a single  $\Delta$ -isobar-hole excitation is

$$\Pi_\Delta^{(0)}(k) = -\left(\frac{f_\pi^*}{m_\pi}\right)^2 \frac{16}{9} k^2 \Gamma_\Delta^2(k) U_\Delta(k), \quad (4.7)$$

where

$$U_\Delta(k) = 2 \int \frac{d^3p}{(2\pi)^3} \frac{1}{\epsilon_p - \epsilon_{|\vec{p}-\vec{k}|} - \omega_\Delta}. \quad (4.8)$$

The energy denominator in the last equation contains the difference between an isobar energy and a nucleon hole energy and therefore depends on the shift  $V_0$  of Eq. (3.1) for the hole energy. In the calculation  $V_0 = 100 \text{ MeV}$  has been used, a value typically obtained in Brueckner calculations. From our numerical calculation we get  $\Pi_N$  and  $\Pi_\Delta$  according to Eq. (2.28). Therefore, since we already determined  $\gamma_N$  as a function of  $k$ , we can extract  $\gamma_\Delta$  and  $\gamma_{\Delta\Delta}$  by requesting that Eqs. (4.4) and (4.5) give the same values for  $\Pi_N$  and  $\Pi_\Delta$  as obtained from the complete calculation. The results of this analysis are displayed in Fig. 14 for  $k_F = 1.40 \text{ fm}^{-1}$  and in Fig. 15 for  $k_F = 1.77 \text{ fm}^{-1}$  as a function of the pion momentum. In addition we have plotted a  $\gamma_{av}$  which can be extracted from the

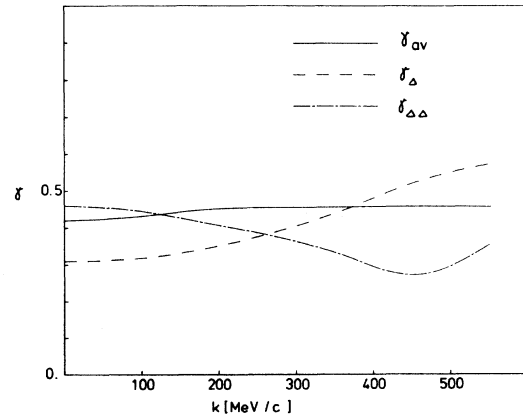


FIG. 14. Effective interaction strengths  $\gamma_\Delta$  (dashed curve) and  $\gamma_{\Delta\Delta}$  (dashed-dotted curve) as obtained from analyzing the self-energy according to Eqs. (4.4) and (4.5). The solid curve represents  $\gamma_{av}$  which is obtained with the assumption  $\gamma_{av} = \gamma_N = \gamma_\Delta = \gamma_{\Delta\Delta}$  [see Eq. (4.9)]. The calculations are performed for  $k_F = 1.4 \text{ fm}^{-1}$  using the Reid soft core potential.

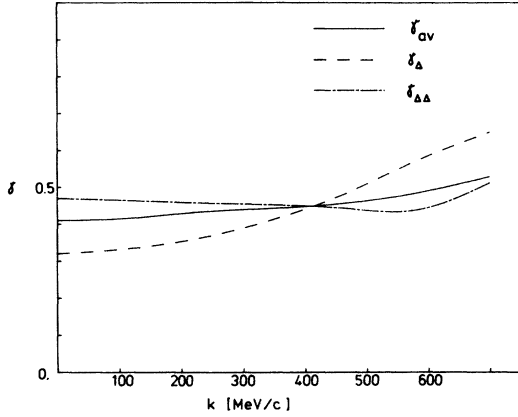


FIG. 15. Effective interaction strengths at  $k_F=1.77 \text{ fm}^{-1}$ . For further details see Fig. 14.

calculated total self-energy under the assumption  $\gamma_N = \gamma_\Delta = \gamma_{\Delta\Delta}$  which is frequently used.<sup>8</sup> Under this assumption the total self-energy  $\Pi$  reduces to

$$\Pi(k) = [\Pi_N^{(0)}(k) + \Pi_\Delta^{(0)}(k)] / \{1 - \gamma_{av}[\Pi_N^{(0)}(k) + \Pi_\Delta^{(0)}(k)/k^2]\}. \quad (4.9)$$

Therefore we can extract  $\gamma_{av}$  when we request Eq. (4.9) to reproduce the calculated value for  $\Pi(k)$ .

For both densities we see that  $\gamma_\Delta$  roughly starts at the value  $\frac{1}{3}$  as a function of the pion momentum, which coincides with the strength of the  $\delta$  function of the exchange part of OPE as discussed in Sec. IIIB. As  $k$  increases,  $\gamma_\Delta$  also increases in both cases due to the increasing importance of the exchange part of  $\rho$  contribution. The bare transition potential should give only a small contribution to  $\gamma_{\Delta\Delta}$ . This can be understood by looking at the details of the ph transformation for single  $\pi$  and  $\rho$ -exchange interactions (see Appendix A). By inspecting the recoupling brackets (A27) we see that the ph transformation leads to a large contribution from the exchange part if only one  $\Delta$  is involved ( $\Delta h$ -ph). The exchange parts are small if only nucleons or two isobars are involved. We remark here again that for bare transition potentials only the exchange pieces of  $\pi$  and  $\rho$  contribute because the direct piece of OPE has to be subtracted and the direct piece of  $\rho$  exchange is not compatible with the pion channel quantum numbers ( $S=1, M_S=0, T=1$ ).

Finally, we see that the curves for  $\gamma_{av}$  show for both densities a rather flat behavior with a value which lies between 0.4 and 0.5, which is at the lower limit of assumptions made in other investigations.

## V. SUMMARY AND CONCLUSION

The aim of this paper has been to check some of the assumptions commonly made when determining the threshold density for pion condensates in nuclear matter. The assumptions concern the irreducible interaction blocks in the nucleon particle-hole ( $NN$ - $NN$ ) and the  $\Delta$ -isobar nucleon-hole ( $\Delta N$ - $\Delta N$ ) channel as well as the interaction ( $NN$ - $\Delta N$ ) coupling both channels. These interactions are complicated functions of three momenta, one energy, and the nuclear density, in general, but are usually replaced in a simple model frame by constant interaction parameters  $\gamma_N$ ,  $\gamma_{\Delta\Delta}$ , and  $\gamma_\Delta$ , respectively, and are often even assumed to be equal,  $\gamma_{av} \equiv \gamma_N = \gamma_{\Delta\Delta} = \gamma_\Delta$ . It should be realized that the threshold density for pion condensation depends sensitively on these interactions.

We have, therefore, checked the model assumptions by constructing the interactions explicitly in terms of a Brueckner  $G$  matrix ( $NN$ - $NN$ ) and  $\pi$  and  $\rho$  meson exchange potentials, modified due to  $NN$  correlations, in the ( $NN$ - $N\Delta$ ) and ( $\Delta N$ - $\Delta N$ ) channels. The present investigation goes beyond the earlier work by Bäckman and Weise<sup>18</sup> in that it keeps the full complexity of the interactions and solves the coupled integral equations for the pion self-energy numerically. Also, different choices for the particle and hole energies are studied, and the symmetries of the interactions in the pion channel are discussed in detail. The numerical results have then finally been interpreted in terms of the simple model of constant interactions, requesting that this model reproduces the self-energies calculated for the realistic interaction. This determines effective parameters  $\gamma_N$ ,  $\gamma_\Delta$ , and  $\gamma_{\Delta\Delta}$  which depend on the pion channel momentum  $k$  and on the nuclear density  $\rho$ . Results are obtained for two densities ( $k_F = 1.40 \text{ fm}^{-1}$  and  $k_F = 1.77 \text{ fm}^{-1}$ ) and two realistic  $NN$  potentials [Reid,<sup>19</sup>  $HM2 + \Delta$  (Ref. 20)]. It is found that the parameters are similar in size,  $\gamma_N \sim \gamma_\Delta \sim \gamma_{\Delta\Delta} = \gamma_{av}$ , and that  $\gamma_{av}$  is only weakly dependent on  $k$  and  $\rho$ . In the region of the critical momentum  $k \sim k_F$ , the results are almost equal for the Reid and the OBE potential. Concerning the  $k$  dependence of  $\gamma_N$ , it is found that the contribution from central interaction decreases with increasing  $k$  at almost the same rate as the contribution from tensor interaction increases keeping the sum almost constant.

It should be realized that the approximations made in the present work, e.g., taking the bare reaction matrix for the nucleon ph channel, hardly account for the full irreducible interactions.<sup>26,27</sup> Therefore attention should be paid to the general results concerning the functional dependence of the parameters on  $k$  and  $\rho$  rather than their absolute

values. With  $\gamma_{av} \sim 0.4-0.5$  extracted here and the self-consistent,  $\rho$ -dependent effective mass (compare Sec. III A), pion condensation is obtained at about twice the normal nuclear density. However, empirical nuclear data indicate that the effective interaction is more repulsive ( $\gamma_{av} \sim 0.7 \pm 0.1$ ), shifting the threshold density to considerably higher values.<sup>14</sup> The importance of the present investigation lies in the fact that it confirms the general assumptions of the simple pion condensation model and it therefore establishes a more solid basis for an empirical analysis of pion condensation based on extrapolation from data at normal nuclear density in the framework of this model.

#### ACKNOWLEDGMENTS

One of us (W.H.D.) would like to thank Dr. E. Boeker for excellent working conditions at the Vrije Universiteit. Part of this investigation was sponsored by the Stichting voor Fundamenteel Onderzoek der Materie (FOM), which is financially supported by the Nederlandse Organisatie voor Zuiver Wetenschappelijk Onderzoek (ZWO).

#### APPENDIX A: THE PARTICLE-HOLE TRANSFORMATION

In this appendix, the transformation of the two body interaction from the particle-particle (pp) into the particle-hole (ph) channel is derived, and symmetry properties are discussed.

In Fig. 16,  $2\vec{Q}$  denotes the two-particle momentum flowing vertically in the pp channel, and  $\vec{k}$  denotes the ph momentum flowing in the ph channel from left to right. Matching momenta of the individual lines, one obtains the relative pp momenta  $\vec{q}_1$  and  $\vec{q}_2$  from the relative ph momenta  $\vec{p}_1$  and  $\vec{p}_2$ ,

$$\vec{q}_1 = \frac{\vec{p}}{2} + \frac{\vec{k}}{2}, \quad \vec{q}_2 = \frac{\vec{p}}{2} - \frac{\vec{k}}{2}, \quad (\text{A1})$$

where  $\vec{p} = \vec{p}_1 - \vec{p}_2$  and

$$\vec{Q} = (\vec{p}_1 + \vec{p}_2)/2. \quad (\text{A2})$$

Choosing the direction of  $\vec{k}$  as the  $z$  axis, polar coordinates are introduced:

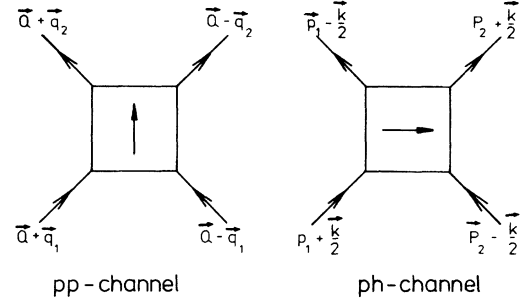


FIG. 16. Particle-particle (pp channel) and particle-hole momenta (ph channel).

$$\vec{p}_{1,2} = (p_{1,2}, \theta_{1,2}, \phi_{1,2}), \quad (\text{A3})$$

$$\vec{q}_{1,2} = (q_{1,2}, \vartheta_{1,2}, \varphi_{1,2}),$$

and relations (A1) are expressed by

$$q_{1,2}^2 = \frac{1}{4} [k^2 + p^2 \pm 2k(p_1 \cos \theta_1 - p_2 \cos \theta_2)], \quad (\text{A4})$$

$$\cos \vartheta_{1,2} = \frac{1}{2q_{1,2}} (p_1 \cos \theta_1 - p_2 \cos \theta_2) \pm \frac{k}{2q_{1,2}}. \quad (\text{A5})$$

Since the  $z$  axis is parallel to  $\vec{k}$ , we have  $\varphi_1 = \varphi_2 = \varphi$ , where  $\varphi$  is the azimuthal angle of  $\vec{p}$ , and this yields

$$\begin{aligned} \tan(\varphi_1) &= \tan(\varphi_2) = \tan(\varphi) \\ &= \frac{p_1 \sin \theta_1 \sin \phi_1 - p_2 \sin \theta_2 \sin \phi_2}{p_1 \sin \theta_1 \cos \phi_1 - p_2 \sin \theta_2 \cos \phi_2}. \end{aligned}$$

If we now rotate around the  $z$  axis with an angle  $\frac{1}{2}(\phi_1 + \phi_2)$ , this becomes

$$\begin{aligned} \tan[\varphi - \frac{1}{2}(\phi_1 + \phi_2)] \\ = \frac{p_1 \sin \theta_1 + p_2 \sin \theta_2}{p_1 \sin \theta_1 - p_2 \sin \theta_2} \tan[\frac{1}{2}(\phi_1 - \phi_2)]. \quad (\text{A6}) \end{aligned}$$

The spins in pp channels are coupled to

$$\begin{aligned} |(s_{p_1} s_{p_2}) sm\rangle &= \sum_{m_{p_1}, m_{p_2}} \langle s_{p_1} m_{p_1}, s_{p_2} m_{p_2} | sm \rangle |s_{p_1} m_{p_1}\rangle \\ &\quad \times |s_{p_2} m_{p_2}\rangle \end{aligned}$$

and in ph channels to

$$\begin{aligned} |(s_p s_h) SM\rangle &= \sum_{m_p, m_h} \langle s_p m_p, s_h m_h | SM \rangle |s_p m_p\rangle (-)^{s_h + m_h} \\ &\quad \times |s_h - m_h\rangle. \end{aligned}$$

Isospins are coupled in the same way. The transformation of the  $G$  matrix has then the form

$$\begin{aligned} \langle (t_1 t_2) T, (s_1 s_2) SM | G^{ph}(\vec{p}_1, \vec{p}_2; k) | (t_3 t_4) T, (s_3 s_4) S'M' \rangle \\ = \sum_t (-)^{t_2 + t_3 + t_4} (2t+1) \begin{Bmatrix} t_1 & t_2 & T \\ t_3 & t_4 & t \end{Bmatrix} \sum_{sm, s'm'} \{ (s_1 s_2) SM, (s_3 s_4) S'M' | (s_1 s_4) sm, (s_2 s_3) s'm' \} \\ \times \langle (t_1 t_4) t, (s_1 s_4) sm | G^{pp}(\vec{q}_1, \vec{q}_2; Q) | (t_2 t_3) t, (s_2 s_3) s'm' \rangle, \quad (\text{A7}) \end{aligned}$$

with the spin transformation bracket

$$\{(s_1 s_2)SM, (s_3 s_4)S'M' | (s_1 s_4)sm, (s_2 s_3)s'm'\} = \sum_{m_1 m_2 m_3 m_4} (-)^{s_2 - m_2} \langle s_1 m_1, s_2 - m_2 | SM \rangle (-)^{s_4 - m_4} \langle s_3 m_3, s_4 - m_4 | S'M' \rangle \times \langle s_1 m_1, s_4 m_4 | sm \rangle \langle s_2 m_2, s_3 m_3 | s'm' \rangle. \quad (\text{A } 8)$$

Using the relations of the Clebsch-Gordan coefficients

$$\langle s_1 m_1, s_2 m_2 | sm \rangle = (-)^{s_1 + s_2 - s} \langle s_2 m_2, s_1 m_1 | sm \rangle = (-)^{s_1 + s_2 - s} \langle s_1 - m_1, s_2 - m_2 | s - m \rangle$$

one finds the symmetry

$$\{(s_1 s_2)SM, (s_3 s_4)S'M' | (s_1 s_4)sm, (s_2 s_3)s'm'\} = (-)^{S + S' + M + M' + s + s' + s_1 + s_2 + s_3 + s_4} \times \{(s_2 s_1)SM, (s_4 s_3)S'M' | (s_2 s_3)s' - m', (s_1 s_4)s - m\}. \quad (\text{A } 9)$$

Also, these brackets vanish unless  $M - M' = m - m'$ .

Since the interaction conserves isospin, the brackets (A8) can be summed to give the 6j symbol in Eq. (A7) for the case of isospin. This is not possible for the spin case, since the interaction couples different spin channels, in general. In the following, we shall not write all the isospin indices and summations explicitly, for convenience; they are easily restored in the final formulas. On the other hand, we shall keep the individual spin indices  $s_1, s_2, s_3,$  and  $s_4$  to allow for nucleons ( $s = \frac{1}{2}$ ) as well as for isobars ( $s = \frac{3}{2}$ ) and their various combinations.

The pp interaction as obtained from a Brueckner calculation is given in a partial wave representation

$$\langle sm | G^{pp}(\vec{q}_1, \vec{q}_2; Q_{av}) | s'm' \rangle = \sum_{JM} \sum_{l m_l, l' m_l'} \langle l m_l, sm | JM \rangle \langle l' m_l', s'm' | JM \rangle Y_{l m_l}(\vartheta_1 \varphi_1) Y_{l' m_l'}^*(\vartheta_2 \varphi_2) G_{l s, l' s'}^J(q_1, q_2; Q_{av}), \quad (\text{A } 10)$$

where  $s$  and  $s'$  stand for  $(s_1 s_4)s$  and  $(s_2 s_3)s'$ , respectively; and the weak dependence on the center-of-mass momentum  $\vec{Q}$  is taken into account only by an average value  $Q_{av}$ . Again we note that  $\varphi_1 = \varphi_2 = \varphi$  and  $m_l - m_l' = m' - m = M' - M$  [see Eq. (A8)]. This implies that one can extract in Eq. (A10) a factor  $\exp[i(M' - M)\varphi]$  which is independent of the summation variables.

The partial wave amplitudes  $G_{l s, l' s'}^J$  satisfy the symmetry

$$G_{l s, l' s'}^J(q_1, q_2; Q_{av}) = G_{l' s', l s}^J(q_2, q_1; Q_{av}). \quad (\text{A } 11)$$

Now, in the integral equation (2.12), the ph interaction is needed for the momenta  $\vec{p}_1, \vec{p}_2$  as well as for the momenta

$$U_{\vec{p}_1} = (p_1, \pi - \theta_1, \phi_1), \quad U_{\vec{p}_2} = (p_2, \pi - \theta_2, \phi_2), \quad (\text{A } 12)$$

which transform into pp momenta

$$\vec{q}_1^u \equiv \vec{q}_1(U_{\vec{p}_1, 2}) = (q_2, \pi - \vartheta_2, \varphi_2), \quad \vec{q}_2^u \equiv \vec{q}_2(U_{\vec{p}_1, 2}) = (q_1, \pi - \vartheta_1, \varphi_1), \quad (\text{A } 13)$$

according to the relations (A4)–(A6). Taking into account Eqs. (A11)–(A13) and noting the symmetry of spherical harmonics

$$Y_{l m}(\pi - \vartheta, \varphi) = (-)^l Y_{l -m}^*(\vartheta, \varphi),$$

one obtains from Eq. (A10) after relabeling summation indices

$$\langle sm | G^{pp}(\vec{q}_1^u, \vec{q}_2^u; Q_{av}) | s'm' \rangle = (-)^{s+s'} \langle s' - m' | G^{pp}(\vec{q}_1, \vec{q}_2; Q_{av}) | s - m \rangle \quad (\text{A } 14)$$

Inserting Eqs. (A9) and (A14) into Eq. (A7), an important symmetry relation for the ph interaction

$$\langle (t_2, t_1)T, (s_2 s_1)SM | G^{ph}(U_{\vec{p}_1}, U_{\vec{p}_2}; k) | (t_4, t_3)T, (s_4 s_3)S'M' \rangle = (-)^{S+S'+M+M'} \times \langle (t_1 t_2)T, (s_1 s_2)SM | G^{ph}(\vec{p}_1, \vec{p}_2; k) | (t_3 t_4)T, (s_3 s_4)S'M' \rangle \quad (\text{A } 15)$$

is obtained. Here we have restored the isospin dependence giving an additional phase  $(-)^{t_1 + t_2 + t_3 + t_4}$  which cancels with the spin phase  $(-)^{s_1 + s_2 + s_3 + s_4}$ . For nucleons with spins  $s = \frac{1}{2}$  only and the pion channel ( $S = S' = 1, M = M' = 0$ ), Eq. (A15) is identical with the symmetry relation (2.14).

In this section, it is shown that the ph interaction depends on the azimuthal angles  $\phi_1$  and  $\phi_2$  only through the difference  $\phi_1 - \phi_2$  and that, accordingly, the integral equation (2.12) separates into  $\phi$ -channels.

Inserting Eq. (A10) into Eq. (A7), one obtains the ph interaction in the form

$$\langle SM | G^{\text{ph}}(\vec{p}_1, \vec{p}_2; k) | S'M' \rangle = \exp(-iM\phi_1 + iM'\phi_2) \times G_{SM, S'M'}(p_1\theta_1, p_2\theta_2, \phi_1 - \phi_2; k) \quad (\text{A16})$$

with

$$\begin{aligned} G_{SM, S'M'}(p_1\theta_1, p_2\theta_2, \phi_1 - \phi_2; k) &= \exp \left[ -i(M - M')\bar{\varphi} + i\frac{M + M'}{2}(\phi_1 - \phi_2) \right] \\ &\times \sum_{sm, s'm'} \{ (s_1s_2)SM, (s_3s_4)S'M' | (s_1s_4)sm, (s_2s_3)s'm' \} \\ &\times \sum_{JM} \sum_{l'm_1, l'm'_1} \langle lm_1, sm | JM \rangle \langle l'm'_1, s'm' | JM \rangle \frac{[(2l+1)(2l'+1)]^{1/2}}{4\pi} \\ &\times d_{0m_1}^{(l)}(\vartheta_1) d_{0m'_1}^{(l')}(\vartheta_2) G_{is, i's'}^J(q_1, q_2; Q_{2\nu}). \end{aligned} \quad (\text{A17})$$

Here the full spin indices for the  $G$  elements would be  $(s_1s_2)S$ ,  $(s_3s_4)S'$ ,  $(s_1s_4)s$ , and  $(s_2s_3)s'$ , respectively, but are not written explicitly, for convenience. According to Eqs. (A4) and (A5), the variables  $q_1$ ,  $\vartheta_1$ ,  $q_2$ , and  $\vartheta_2$  in the pp channel depend on  $\phi_1$  and  $\phi_2$  only through  $(\phi_1 - \phi_2)$ . The azimuthal angle  $\varphi = \varphi_1 = \varphi_2$  has been isolated in Eq. (A17), using  $Y_{lm}(\vartheta, \varphi) = [(2l+1)/4\pi]^{1/2} d_{0m}^{(l)}(\vartheta) \exp(im\varphi)$  and the selection rules of the transformation brackets. This yields the phase

$$\begin{aligned} \exp[-i(M - M')\varphi] &= \exp(-iM\phi_1 + iM'\phi_2) \\ &\times \exp \left[ -i(M - M')\bar{\varphi} \right. \\ &\quad \left. + i\frac{M + M'}{2}(\phi_1 - \phi_2) \right], \end{aligned}$$

where the angle  $\bar{\varphi} = \varphi - (\phi_1 + \phi_2)/2$  also is a function of  $(\phi_1 - \phi_2)$  alone, according to Eq. (A6).

The interaction (A17) is periodic in  $(\phi_1 - \phi_2)$  over a period of  $2\pi$  except for the phase  $\exp[i(M + M') \times (\phi_1 - \phi_2)/2]$  which is periodic over  $4\pi$ , in general. We therefore define the Fourier transforms

$$\begin{aligned} G_{SM, S'M'}^{(n)}(p_1\theta_1, p_2\theta_2; k) \\ = \int_0^{4\pi} \frac{d(\phi_1 - \phi_2)}{4\pi} e^{in(\phi_1 - \phi_2)/2} \\ \times G_{SM, S'M'}(p_1\theta_1, p_2\theta_2, \phi_1 - \phi_2; k) \end{aligned} \quad (\text{A18})$$

which satisfy the selection rule

$$G_{SM, S'M'}^{(n)} = 0$$

if  $n + M + M'$  is an odd integer.

Due to the  $(\phi_1 - \phi_2)$  dependence of the interactions (A16), it is now obvious that the integral equation (2.12) can be decomposed into  $\phi$  channels ( $n = 0, \pm 1, \pm 2, \dots$ ). The interaction appears in the combination

$$\begin{aligned} K_{TSM, TSM'}^{(n)}(p_1\theta_1, p_2\theta_2; k) &= G_{TSM, TSM'}^{(n)}(p_1\theta_1, p_2\theta_2; k) \\ &\quad - (-)^{S+M'} G_{TSM, TSM'}^{(n)} \\ &\quad \times (p_1\theta_1, p_2(\pi - \theta_2); k), \end{aligned} \quad (\text{A19})$$

where we have again written the isospin dependence explicitly. The elements  $K^{(n)}$  obey the symmetries

$$\begin{aligned} K_{TSM, TSM'}^{(n)}(p_1(\pi - \theta_1), p_2(\pi - \theta_2); k) \\ = (-)^{S+M+S'+M'} K_{TSM, TSM'}^{(n)}(p_1\theta_1, p_2\theta_2; k), \end{aligned} \quad (\text{A20})$$

$$\begin{aligned} K_{TSM, TSM'}^{(n)}(p_1\theta_1, p_2\theta_2; k) \\ = (-)^{S+M+S'+M'} K_{TS-M, TS-M'}^{(-n)}(p_1\theta_1, p_2\theta_2; k), \end{aligned}$$

and vanishes if  $(n + M + M')$  is odd (see above).

Only the  $n = 0$  channel can contribute to the pion self-energy in Eq. (2.1). Since the pion channel is ( $S = 1, M = 0$ ) the interaction  $K$  only couples to channels with  $M'$  even. Using the symmetry relation (A20), which yields e.g.,  $K_{TS0, TS0}^{(0)} = 0$  for  $S + S'$  odd, it can be seen that the only channels to be considered are those with ( $S = 1, M = 0$ ) and ( $S = 2, M = \pm 2$ ). Therefore for the case of nucleons only ( $S, S' \leq 1$ ) the pion channel couples only to itself.

ph transformation for single  $\pi$ - or  $\rho$ -exchange interaction

We start by noting that a  $\pi$ - or  $\rho$ -exchange interaction can be decomposed in a tensor and a central part. It is important to make this decomposition otherwise one has to use the more general ph-transformation discussed above. We first give the general form of the interaction for  $\pi$  exchange:

$$\begin{aligned} V^{\pi}(\vec{q}) &= -\frac{f_{\pi}^1 f_{\pi}^2}{m_{\pi}^2} \Gamma_{\pi}^1(q) \Gamma_{\pi}^2(q) \frac{\vec{\xi}_1 \cdot \vec{q} \vec{\xi}_2 \cdot \vec{q}}{m_{\pi}^2 + q^2} \vec{\tau}_1 \cdot \vec{\tau}_2 \\ &= -\frac{f_{\pi}^1 f_{\pi}^2}{m_{\pi}^2} \Gamma_{\pi}^1(q) \Gamma_{\pi}^2(q) \frac{1}{3} q^2 \frac{[\xi_{12}(\hat{q}) + \vec{\xi}_1 \cdot \vec{\xi}_2]}{m_{\pi}^2 + q^2} \vec{\tau}_1 \cdot \vec{\tau}_2, \end{aligned} \quad (\text{A21})$$

and for  $\rho$  exchange:

$$V^\rho(\vec{q}) = -\frac{f_\rho^1 f_\rho^2}{m_\rho^2} \Gamma_\rho^1(q) \Gamma_\rho^2(q) \frac{(\vec{\xi}_1 \times \vec{q}) \cdot (\vec{\xi}_2 \times \vec{q})}{m_\rho^2 + q^2} \vec{\tau}_1 \cdot \vec{\tau}_2$$

$$= -\frac{f_\rho^1 f_\rho^2}{m_\rho^2} \Gamma_\rho^1(q) \Gamma_\rho^2(q) \frac{1}{3} q^2 \frac{[-\xi_{12}(\hat{q}) + 2\vec{\xi}_1 \cdot \vec{\xi}_2]}{m_\rho^2 + q^2} \vec{\tau}_1 \cdot \vec{\tau}_2,$$
(A22)

where  $f_\rho^i$  ( $f_\rho^i$ ) and  $\Gamma_\rho^i(q)$  [ $\Gamma_\rho^i(q)$ ] denote the  $\pi$  ( $\rho$ ) baryon-baryon coupling constant and form factor for vertex  $i$  and

$$\xi_{12}(\hat{q}) = 3\vec{\xi}_1 \cdot \hat{q} \vec{\xi}_2 \cdot \hat{q} - \vec{\xi}_1 \cdot \vec{\xi}_2$$

$$= [24\pi]^{1/2} \sum_\mu (2\mu 2 - \mu | 00) [\vec{\xi}_1 \times \vec{\xi}_2]_\mu {}^2 Y_{2,\mu}(\hat{q}).$$
(A23)

The momentum of the exchanged pion (rho meson) is  $\vec{q}$ . The operators  $\vec{\xi}_i$  and  $\vec{\tau}_i$  stand for the various spin and isospin operators connected with vertex  $i$ . These operators are  $\vec{\sigma}(\vec{\tau})$ ,  $\vec{S}(\vec{T})$ , and  $\vec{S}^*(\vec{T}^*)$ , which have the following reduced matrix elements:

$$\langle \frac{1}{2} \| \vec{\sigma} \| \frac{1}{2} \rangle = \langle \frac{1}{2} \| \vec{\tau} \| \frac{1}{2} \rangle = \sqrt{6},$$

$$\langle \frac{3}{2} \| \vec{S} \| \frac{1}{2} \rangle = \langle \frac{3}{2} \| \vec{T} \| \frac{1}{2} \rangle = 2,$$
(A24)

$$\langle \frac{1}{2} \| \vec{S}^* \| \frac{3}{2} \rangle = \langle \frac{1}{2} \| \vec{T}^* \| \frac{3}{2} \rangle = -2.$$

In contrast to the general ph transformation one can keep track of direct and exchange contributions. To make this point clear, let us consider the first step of the ph transformation

$$\langle (b_1 b_2^{-1}) S M_S T M_T | V^{\text{ph}} | (b_3 b_4^{-1}) S' M'_S T M_T \rangle$$

$$= \sum_{\sigma_i, \tau_i} (-)^{s_2 - \sigma_2} (s_1 s_1 s_2 - \sigma_2 | S M_S) (-)^{t_2 - \tau_2} (t_1 t_1 t_2 - \tau_2 | T M_T) (-)^{s_4 - \sigma_4} (s_3 s_3 s_4 - \sigma_4 | S' M'_S) (-)^{t_4 - \tau_4} (t_3 t_3 t_4 - \tau_4 | T M_T)$$

$$\times \langle s_1 \sigma_1 t_1 \tau_1, s_4 \sigma_4 t_4 \tau_4 | V^{\text{pp}} | s_2 \sigma_2 t_2 \tau_2, s_3 \sigma_3 t_3 \tau_3 \rangle_{\text{a.s.}},$$
(A25)

where a.s. (antisymmetry) means that one has to consider the identity or nonidentity of baryon 1 and 4 and of baryon 2 and 3. The following pp matrix elements are then possible:

(1) For  $b_1 = b_4$ ,  $b_2 = b_3$ , either

$$\langle s_1 \sigma_1 t_1 \tau_1, s_4 \sigma_4 t_4 \tau_4 | V^{\text{pp}} \{ | s_2 \sigma_2 t_2 \tau_2, s_3 \sigma_3 t_3 \tau_3 \rangle - | s_3 \sigma_3 t_3 \tau_3, s_2 \sigma_2 t_2 \tau_2 \rangle \}$$
(i)

or

$$\{ \langle s_1 \sigma_1 t_1 \tau_1, s_4 \sigma_4 t_4 \tau_4 | - \langle s_4 \sigma_4 t_4 \tau_4, s_1 \sigma_1 t_1 \tau_1 | \} V^{\text{pp}} | s_2 \sigma_2 t_2 \tau_2, s_3 \sigma_3 t_3 \tau_3 \rangle,$$
(ii)

where the exchange also influences the momentum dependence. (i) and (ii) are equivalent here.

(2)  $b_1 = b_4$ ,  $b_2 \neq b_3$ . In this case one has matrix elements (ii).

(3)  $b_1 \neq b_4$ ,  $b_2 = b_3$ . In this case one has matrix elements (i).

(4) For  $b_1 \neq b_4$ ,  $b_2 \neq b_3$ , either

$$\langle s_1 \sigma_1 t_1 \tau_1, s_4 \sigma_4 t_4 \tau_4 | V^{\text{pp}} | s_2 \sigma_2 t_2 \tau_2, s_3 \sigma_3 t_3 \tau_3 \rangle$$
(iii)

or

$$- \langle s_1 \sigma_1 t_1 \tau_1, s_4 \sigma_4 t_4 \tau_4 | V^{\text{pp}} | s_3 \sigma_3 t_3 \tau_3, s_2 \sigma_2 t_2 \tau_2 \rangle$$
(iv)

depending on the interaction.

It is clear that in cases 1, 2, and 3 one has a direct and an exchange contribution, while in case 4 one either has a "direct" piece or an "exchange" piece. The actual formulas can be derived using standard angular momentum recoupling techniques for the spin and isospin parts of the interaction. For the tensor piece one gets the following reduced matrix element:

$$\langle (s_1 s_2^{-1}) S \| [\vec{\xi}_1 \times \vec{\xi}_2]^2 \| (s_3 s_4^{-1}) S' \rangle = \begin{cases} \frac{\sqrt{5}}{3} (-)^{s_4 + s_3} \langle s_1 \| \vec{\xi}_1 \| s_2 \rangle \langle s_4 \| \vec{\xi}_2 \| s_3 \rangle \delta_{s,1} \delta_{s',1} & \text{(direct)} \\ \sqrt{5} (-)^{s_2 + s_4} [(2S+1)(2S'+1)]^{1/2} \langle s_4 \| \vec{\xi}_1 \| s_2 \rangle \langle s_1 \| \vec{\xi}_2 \| s_3 \rangle \begin{Bmatrix} s_1 & s_2 & S \\ s_3 & s_4 & S' \\ 1 & 1 & 2 \end{Bmatrix} & \text{(exchange),} \end{cases}$$
(A26)

where the minus sign for the exchange has not been included. It is sufficient here to give the reduced matrix element because one can apply the Wigner-Eckart theorem. We use here the definition of the reduced matrix element of Ref. 28. For the central piece one finds

$$\langle (s_1 s_2^{-1}) S M_S | \vec{\xi}_1 \cdot \vec{\xi}_2 | (s_3 s_4^{-1}) S M_S \rangle = \begin{cases} -\frac{1}{3} (-)^{s_3+s_4} \langle s_1 || \vec{\xi}_1 || s_2 \rangle \langle s_4 || \vec{\xi}_2 || s_3 \rangle \delta_{s,1} & \text{(direct)} \\ -(-)^{s_3+s_4+s} \begin{Bmatrix} s_1 & s_2 & S \\ s_4 & s_3 & 1 \end{Bmatrix} \langle s_4 || \vec{\xi}_1 || s_2 \rangle \langle s_1 || \vec{\xi}_2 || s_3 \rangle & \text{(exchange)}. \end{cases} \quad (\text{A27})$$

As an example we will give the ph matrix elements for  $\pi$  exchange for the  $NN \rightarrow N\Delta$  transition potential. Taking the spin quantization axis along the direction of the total momentum  $\vec{k}$ , one gets neglecting form factors for simplicity:

$$\begin{aligned} & \langle k, \vec{p}_1; (\frac{3}{2} \frac{1}{2}^{-1}) S M_S T | V^\tau | k, \vec{p}_2; (\frac{1}{2} \frac{1}{2}^{-1}) S' M_S' T \rangle \\ &= -\frac{f_\tau f_\tau^*}{m_\tau^2} \left[ \delta_{s,1} \delta_{T,1} \delta_{M_S, M_S'} \delta_{M_S, 0} \left( \frac{16}{9} \frac{k^2}{m_\tau^2 + k^2} + \frac{8}{9} \frac{k^2}{m_\tau^2 + k_2^2} \right) \right. \\ & \quad + 8 \frac{(\vec{p}_1 - \vec{p}_2)^2}{m_\tau^2 + (\vec{p}_1 - \vec{p}_2)^2} (-)^{s+M_S'+T} \begin{Bmatrix} S & 2 & S' \\ -M_S & M_S - M_S' & M_S' \end{Bmatrix} (24\pi)^{1/2} Y_{2, M_S - M_S'}(p_1, \hat{p}_2) [(2S+1)(2S'+1)]^{1/2} \\ & \quad \left. \times \begin{Bmatrix} \frac{3}{2} & \frac{1}{2} & 1 \\ \frac{1}{2} & \frac{1}{2} & 1 \end{Bmatrix} \begin{Bmatrix} \frac{3}{2} & \frac{1}{2} & T \\ \frac{1}{2} & \frac{1}{2} & 1 \end{Bmatrix} - \delta_{s, s'} \delta_{M_S, M_S'} 8 \frac{(\vec{p}_1 - \vec{p}_2)^2}{m_\tau^2 + (\vec{p}_1 - \vec{p}_2)^2} (-)^{s+T} \begin{Bmatrix} \frac{3}{2} & \frac{1}{2} & S \\ \frac{1}{2} & \frac{1}{2} & 1 \end{Bmatrix} \begin{Bmatrix} \frac{3}{2} & \frac{1}{2} & T \\ \frac{1}{2} & \frac{1}{2} & 1 \end{Bmatrix} \right]. \quad (\text{A28}) \end{aligned}$$

The terms in the matrix elements with  $k$  come from the direct part, those with  $(\vec{p}_1 - \vec{p}_2)$  from the exchange; both parts have been kept separate with respect to central and tensor pieces (tensor contribution+central in that order).

The last part of Appendix A is devoted to a table of the coupling constants, masses, and cutoff masses which are used in the calculation (Table II). We have taken at each vertex a form factor of the form  $[(\Lambda^2 - m^2)/(\Lambda^2 + k^2)]$ , where  $\Lambda$  is the cutoff mass,  $m$  the mass of the exchanged meson, and  $k$  its momentum. Note that the  $\pi NN$ -coupling constant was taken from the  $HM2 + \Delta$  interaction.

TABLE II. Coupling constants, masses, and cutoff masses (both in MeV) that were used in the calculation.

$f_\tau$	0.978	$f_\rho$	5.416
$f_\tau^*$	1.956	$f_\rho^*$	9.192
$\Lambda_{NN}^*$	1200	$\Lambda_{NN}^\rho$	1800
$\Lambda_{N\Delta}^*$	1200	$\Lambda_{N\Delta}^\rho$	1800
$m_\tau$	139	$m_\rho$	770
$m_N$	938.9	$m_\Delta$	1236

## APPENDIX B: THE AVERAGED STARTING ENERGY

In this appendix the averaged starting energy  $E_0$  to be used in the input  $G$  matrix is derived. Noting that  $G(E)$  is smoothly dependent on  $E$ , we expand

$$G(\epsilon_p + \epsilon_{p'}) = G(E_0) [1 + \alpha(\epsilon_p - E_0/2) + \alpha(\epsilon_{p'} - E_0/2) + \dots] \quad (\text{B1})$$

and determine  $E_0$  in such a way that the self-energy

$$\begin{aligned} \Pi_N(k) &= \int_F \frac{d^3 p}{(2\pi)^3} \tau^{(0)}(k) \frac{1}{\epsilon_p - \epsilon_{|\vec{p} - \vec{k}|}} \\ & \quad \times [\tau(\vec{p} - \vec{k}/2, \epsilon_p; k) + \tau(U(\vec{p} - \vec{k}/2), \epsilon_p; k)] \end{aligned} \quad (\text{B2})$$

does not depend on  $\alpha$  in linear order. Approximately, this is achieved by neglecting all the explicit dependence on  $\vec{p}$  and  $\vec{p}'$  in the ph interaction  $G(\vec{p} - \vec{k}/2, \vec{p}' - \vec{k}/2, k; \epsilon_p + \epsilon_{p'})$ . The integral equation (2.8) for the vertex  $\tau(\vec{p} - \vec{k}/2, \epsilon_p; k)$  then has the form

$$\begin{aligned} \tau(\epsilon_p) &= \tau^{(0)} + 2G(E_0) \left[ 1 + \alpha \left( \epsilon_p - \frac{E_0}{2} \right) \right] \int_F \frac{d^3 p'}{(2\pi)^3} \frac{\tau(\epsilon_{p'})}{\epsilon_{p'} - \epsilon_{|\vec{p}' - \vec{k}|}} \\ & \quad + 2G(E_0) \alpha \int_F \frac{d^3 p'}{(2\pi)^3} \frac{\epsilon_{p'} - E_0/2}{\epsilon_{p'} - \epsilon_{|\vec{p}' - \vec{k}|}} \tau(\epsilon_{p'}). \end{aligned} \quad (\text{B3})$$

Choosing  $E_0$  such that

$$\int_F \frac{d^3p}{(2\pi)^3} \frac{\epsilon_p - E_0/2}{\epsilon_p - \epsilon_{|\vec{p}-\vec{k}|}} = 0, \quad (\text{B4})$$

all the terms of  $\tau(\epsilon_p)$  linear in  $\alpha$  cancel when inserted into Eq. (B2). With  $\epsilon_p = p^2/2m^* - V_0$ ,  $\epsilon_F = p_F^2/2m^*$ , and  $a = k/2p_F$ , one obtains

$$E_0 = 2 \int_F \frac{d^3p}{(2\pi)^3} \frac{\epsilon_p}{\epsilon_p - \epsilon_{|\vec{p}-\vec{k}|}} / \int_F \frac{d^3p}{(2\pi)^3} \frac{1}{\epsilon_p - \epsilon_{|\vec{p}-\vec{k}|}} \\ = \epsilon_F \left( \frac{a^{2+\frac{1}{3}} - \frac{1-a^4}{2a} \ln \left| \frac{1-a}{1+a} \right|}{1 - \frac{1-a^2}{2a} \ln \left| \frac{1-a}{1+a} \right|} \right) - 2V_0. \quad (\text{B5})$$

\*Present address: Projektgruppe für Laserforschung der MPG, D-8046 Garching, West Germany.

<sup>1</sup>O. Maxwell, G. E. Brown, D. K. Campbell, R. F. Dashen, and J. T. Manassah, *Astrophys. J.* **216**, 77 (1977).

<sup>2</sup>A. B. Migdal, A. I. Chernoutsan, and I. N. Mishustin, *Phys. Lett.* **83B**, 158 (1979).

<sup>3</sup>V. Ruck, M. Gyulassy, and W. Greiner, *Z. Phys.* **A277**, 391 (1976); M. Gyulassy and W. Greiner, *Ann. Phys. (N.Y.)* **109**, 485 (1977).

<sup>4</sup>A. B. Migdal, *Phys. Lett.* **65B**, 423 (1976).

<sup>5</sup>J. Meyer-ter-Vehn, *Phys. Rep.* (to be published).

<sup>6</sup>H. Toki and W. Weise, *Phys. Rev. Lett.* **42**, 1034 (1979).

<sup>7</sup>S. A. Fayans, E. E. Saperstein, and S. V. Tolokonnikov, *Nucl. Phys.* **A326**, 463 (1979).

<sup>8</sup>S.-O. Bäckman and W. Weise, in *Mesons in Nuclei*, edited by M. Rho and D. H. Wilkinson (North-Holland, Amsterdam, 1979), p. 1095.

<sup>9</sup>A. B. Migdal, *Zh. Eksp. Teor. Fiz.* **61**, 2210 (1971) [*Sov. Phys.—JETP* **34**, 1184 (1972)]; *ibid.* **63**, 1993 (1972) [*ibid.* **36**, 1052 (1973)].

<sup>10</sup>R. F. Sawyer, *Phys. Rev. Lett.* **29**, 382 (1972); D. J. Scalapino, *ibid.* **29**, 386 (1972); R. F. Sawyer and D. J. Scalapino, *Phys. Rev. D* **7**, 953 (1973).

<sup>11</sup>G. E. Brown and W. Weise, *Phys. Rep.* **27C**, 1 (1976).

<sup>12</sup>A. B. Migdal, *Rev. Mod. Phys.* **50**, 107 (1978).

<sup>13</sup>S. A. Fayans, E. E. Saperstein, and S. V. Tolokonnikov, *J. Phys. G* **3**, L51 (1977).

<sup>14</sup>J. Meyer-ter-Vehn, *Z. Phys.* **A287**, 241 (1978); Pro-

ceedings of the Symposium on Relativistic Heavy Ion Research, GSI Report No. P-5, 302 (1978).

<sup>15</sup>H. Toki and W. Weise, *Z. Phys. A* **292**, 389 (1979).

<sup>16</sup>G. Bertsch and M. B. Johnson, *Phys. Rev. D* **12**, 2230 (1975).

<sup>17</sup>W. Weise and G. E. Brown, *Phys. Lett.* **48B**, 297 (1974).

<sup>18</sup>S.-O. Bäckman and W. Weise, *Phys. Lett.* **55B**, 1 (1975).

<sup>19</sup>R. V. Reid, *Ann. Phys. (N.Y.)* **50**, 411 (1968).

<sup>20</sup>K. Holinde and R. Machleidt, *Nucl. Phys.* **A280**, 429 (1977).

<sup>21</sup>Y. Futami, H. Toki, and W. Weise, *Phys. Lett.* **77B**, 37 (1978).

<sup>22</sup>R. Rajamaran, in *Mesons in Nuclei*, edited by M. Rho and D. H. Wilkinson (North-Holland, Amsterdam, 1979), p. 197.

<sup>23</sup>M. I. Haftel and F. Tabakin, *Nucl. Phys.* **A158**, 1 (1970).

<sup>24</sup>S.-O. Bäckman, A. D. Jackson, and O. Sjöberg, *Nucl. Phys.* **A321**, 10 (1979).

<sup>25</sup>J. W. Durso, M. Saarela, G. E. Brown, and A. D. Jackson, *Nucl. Phys.* **A278**, 445 (1977).

<sup>26</sup>G. E. Brown, *Rev. Mod. Phys.* **43**, 1 (1971).

<sup>27</sup>H. Müther, Y. Waghmare, and A. Faessler, *Z. Phys. A* **294**, 87 (1980).

<sup>28</sup>A. de Shalit and I. Talmi, *Nuclear Shell Theory* (Academic, New York and London, 1963).